Polypyrrole film on 55% Al–Zn-coated steel for corrosion prevention

Haku Ryu*, Nan Sheng*, Toshiaki Ohtsuka* $,

Sakae Fujita#, and Hiroshi Kajiyama#

*Division of Materials Science and Engineering,

Faculty of Engineering, Hokkaido University,

Kita13 Nishi 8, Kita-ku, Sapporo, Hokkaido 060-8628, Japan

#Steel Research Laboratory, JFE Steel Co.,

Kawasaki-cho 1, Chuo-ku, Chiba 260-0835, Japan

$Corresponding author: E- mail ohtsuka@eng.hokudai.ac.jp

Tel & Fax +81-11-706-6351

Abstract

For corrosion protection of 55% Al–Zn-coated steel, a dense polypyrrole (PPy) film is electrochemically formed on 55% Al–Zn-coated steel in an acidic tartrate solution under constant current control. The film potentially consists of an inner layer of aluminium and/ or zinc oxide and an outer PPy layer doped with tartrate anions. The PPy layer can maintain passivation of 55% Al–Zn-coated steel in a 3.5 wt% NaCl aqueous solution and protected the steel for several hours. The doping of molybdate anions into the PPy-tartrate film greatly improved the film's protective properties.

Key Words: C. Corrosion prevention, B. polypyrrole, B. Al–Zn alloy, B. tartrate

1. Introduction

Coating with conductive polymers is a promising method for corrosion protection of metals. Many papers have been published on corrosion protection, and oxidative conducting polymers such as polypyrrole (PPy), polyaniline (PANI), and polythiophen (PThio) are widely used in corrosion protection [1–6]. Anodic protection has been assumed to be the mechanism through which conductive polymers protect against corrosion. [1] Anodic protection occurs when the oxidative action of the polymer coating induces passivation of the substrate metals, and the metals are protected by a thin passive oxide or salt layer located underneath the polymer coating.

A 55% Al–Zn coating has been used for the prevention of steel corrosion, and this coating is sometimes treated by chromate before painting the coating onto the substrate. Because of the environmental problems associated with chromate, it has been replaced by other substitution treatments. The chromate conversion coating has an important advantage in that there is a self-healing property associated with corrosion prevention [7]. The self-healing property of the chromate conversion coating results from the repair of the passive oxide layer at damaged sites. A conductive polymer that is designed to have oxidative action and to include inhibitors against corrosion may be a candidate that can successfully replace chromate [8, 9]. In this study, we utilise electropolymerisation of PPy to place a conductive

polymer coating on a 55% Al–Zn alloy, which is used in corrosion protection of zinc-alloy-coated steel.

Formation of a PPy layer on aluminium for corrosion prevention by electropolymerisation in various aqueous electrolytes and capacitor applications has been previously reported [10–23]. PPy formation on zinc or a zinc-coated steel has also reported to prevent corrosion [8, 24–34].

When coating Zn surfaces with PPy, active dissolution of zinc may prevent oxidised polymerisation of the PPy because sufficiently positive potentials cannot be reached to produce polymerisation of the pyrrole monomer (Py). Therefore, surface passivation treatment or the predeposition of a zinc salt layer may be required for the preparation of PPy coated zinc surfaces. For example, Zaid *et al.* first treated a zinc surface with a NaS solution to make an inert ZnS-ZnO_xH_y surface layer and subsequently initiated the polymerisation of Py [26]. Petitjean *et al.* electrochemically prepared a PPy layer on zinc in an aqueous sodium salicylate solution, where a zinc salicylate salt layer was formed to passivate the zinc surface before polymerisation occurred [24, 25]. Martins *et al.* prepared a PPy layer on zinc in an aqueous tartrate solution, where a zinc tartrate salt layer acted as a passivation layer on the zinc surface [28, 29]. We have also prepared a PPy layer on zinc in an acidic tartrate solution, and we have observed the formation of an oxide and salt layer between the zinc and PPy by cross-sectional analysis using scanning electron microscopy (SEM) [34].

During the preparation of a PPy layer on aluminium, the formation of an anodic oxide may inhibit polymerisation because the applied anodic current can potentially result in the formation of anodic oxide, which would prevent PPy polymerisation from occurring. An anodic oxide that has dielectric properties and little electronic conductivity may suppress PPy polymerisation. For the preparation of PPy coatings, various organic acids and solutions of the acid's correspond salt, such as oxalic acid [12], saccharin [16], malic acid [18], dodecylsulphate [20], dodecylbenzene sulfonate [20], and succinate [19], have been utilised for the successful formation of PPy layers. The above research was performed in either neutral or acidic solutions. Saidman *et al.* successfully prepared a conductive PPy layer in basic solution at pH 12 that contained nitrate and molybdate anions [13-15]. Molybdate anions are well known to be an effective passivator that facilitates passivation of various metals. Paliwoda-Porebska *et al.* reported that a PPy layer doped with molybdate anions potentially acted as a protective layer with self-healing properties [8].

In this paper, we successfully prepared a PPy layer on 55% Al–Zn-coated steel in an acidic tartrate solution under constant current control to protect the coated steel against corrosion. Constant current control was used to control the thickness of the PPy layer. The thickness can be determined by the anodic charge passed by determining, for example, the time period of current control. Corrosion prevention for the 55% Al–Zn-coated steel covered

with a PPy layer was studied by an immersion test in an aqueous sodium chloride solution, linear sweep voltammometry, and electrochemical impedance spectroscopy. The relationship between the corrosion protection properties and the condition of the PPy layer was also examined. Finally, molybdate dopant ions were investigated to determine the effect that these ions have on corrosion protection and to determine how molybdate anions act as an inhibitor in a steel-coating PPy layer.

2. Experimental

Steel sheets that were 0.5 mm thick and coated with a 55% Al–Zn alloy were provided by JFE Steel Co Ltd. The 55% Al–Zn alloy layer was approximately 20 μm thick, and its composition was 55 wt% Al, 43.4 wt% Zn, and 1.6 wt% Si. The sheet was cut to 2.5 x 1.5 cm^2 and then washed in acetone using ultrasonication. The edges of the steel sheet were covered by silicone resin and both faces with areas of 1.0×1.0 cm^2 were used for the PPy polymerisation.

All solutions were prepared from analytical grade reagents and pure deionised water obtained from a Millipore purification system. The aqueous solutions used for the electropolymerisation of PPy were tartaric acid, sodium tartrate, and mixtures of sodium tartrate and tartaric acid. The tartrate ion concentration of all solutions was 0.5 mol dm^{-3} (M). A 5 mM

solution of sodium molybdate was added to the tartrate solutions when the effect of doped molybdate ions was examined. After deaeration of the solution by bubbling pure nitrogen gas through the solution, pure pyrrole (Py) monomer purchased from Tokyo Chemical Industry was added by syringe until a 0.6 M concentration was reached. For electropolymerisation of PPy, a three-electrode cell with 50 cm^3 volume was used, and this cell was connected to the glass flask where the deaerated preparation solution was stored. An Ag/ AgCl/ saturated KCl electrode (SSE) and a platinum sheet were used in the cell for the reference and counter electrodes, respectively. The SSE reference electrode was used for all the electrochemical measurements in this study. Anodic electropolymerisation of PPy was performed under constant current control from 1.0 to 5.0 mA cm^{-2} in the tartrate solutions with a Py monomer concentration of 0.6 M and pH values ranging from 1.5 to 8.4. These electropolymerisations were performed both in the absence and presence of sodium molybdate. The current control and potential measurements were conducted using a Hokuto-Denko HA501 potentiostat.

The formed PPy layer was analysed by Raman spectroscopy (RS) and infrared reflection absorption spectroscopy (IR-RAS). For RS, a Bunko-Keiki M30-TP-M polychromator spectrometer with a 300 mm optical length and a holographic grating with 1200 grooves mm^{-1} was used. The spectrometer was equipped with a highly sensitive CCD detector (Andor DU401A) and a

100 mW-power YVO_4 solid-state laser with a wavelength of 532 nm. The excitation for RS was performed using laser light with a power of 1 mW at an incidence angle of 60°, and Raman scattering light from the PPy layer covering the 55% Al–Zn coated steel was collected in the direction normal to the steel surface with a confocal optical system. For IR-RAS, a JASCO FT-IR 4000 instrument was used, which is equipped with a CMT detector and a grazing angle measurement accessory, JASCO RAS PO410-H, with an incidence angle of 85°.

A JEOL JXA-8900M SEM was used to observe the surface of the PPy layer coating the steel substrates. The elemental depth profile was measured by glow discharge optical emission spectroscopy (GD-OES) using a Horiba JY-5000 RF spectrometer.

A Laser Tech 1LM21D confocal laser scanning microscope was used to measure the thickness of the PPy layer formed on the steel samples. The step distance between the coated region of the PPy layer and the uncoated surface was used to estimate the layer thickness.

The protective properties of the PPy layer formed on the alloy coated steel with an anodic charge of 3.0–5.0 C cm^{-2} at various current densities (CDs) were examined by immersing the coated steel into an aqueous 3.5 wt% sodium chloride solution at a temperature of 25 ± 0.5 °C under atmospheric conditions. The immersion test was performed in a cylindrical glass flask with a 150 cm^3 volume in which the 55% Al–Zn-coated steel plate covered by

a PPy layer was fixed by an electric lead wire, and a SSE reference electrode was inserted. During immersion, the open circuit potential (OCP) or the corrosion potential of the 55% Al–Zn steel covered by the PPy layer was monitored against the SSE by a Hokuto-Denko HE-104 potentiometer and a Graphtec Midi Logger GL-450 data logger. The formation of corrosion products was also observed by visual inspection. In addition to the immersion test, linear sweep voltammogram and electrochemical AC impedance spectroscopy (EIS) of the 55% Al–Zn-coated steel covered by the PPy layer were measured by a three-electrode system in a glass cell with 100 cm^3 volume equipped with a SSE reference electrode and a Pt sheet counter electrode. The measurement of linear sweep voltammogram was performed by a Hokuto Denko HZ-5000 potentiostat, and EIS was measured from 10^{-2} to 10^4 Hz with a 0.01 V amplitude by a frequency response analyser (FRA), NF Circuit Design 5020, that was connected to a potentiostat specially designed in our laboratory.

The AC impedance spectroscopy of 55% Al–Zn-coated steel covered by PPy was also measured under dry conditions after the PPy layer was dried in a desiccator. For this measurement, two gold disc plates with diameters of 10 mm were used as electric contact probes, and these probes were pressed by springs to both sides of the coated steel covered by the PPy layer.

3. Results

3.1 Effect of sodium tartrate and tartaric acid mixture ratio

The ratio of sodium tartrate and tartaric acid greatly affected the potential of PPy polymerisation under constant current. Figure 1 shows the potential change during the constant current polymerisation at 5.0 mA cm^{-2} in solutions of 0.5 M sodium tartrate at pH 8.4, 0.5 M tartaric acid at pH 1.5, and a 92:8 molar mixture of 0.5 M tartaric acid and 0.5 M sodium tartrate at pH 2.1. All solutions contained 0.6 M Py monomer. After oxidation for 600 s, a black PPy layer was observed on the 55% Al–Zn-coated steel. In the acidic tartrate solution, the potential initially increased sharply from the initial immersion potential of −1.6 V (vs. Ag/AgCl/saturated KCl (SSE)) until the potential peaked at 2.6 V after 5 s, and subsequently, the potential gradually decreased to a constant value. The initial increase in potential may correspond to the growth of an oxide and nucleation of PPy on the 55% Al–Zn alloy. The subsequent potential decrease may correspond to the three-dimensional growth of the PPy layer. In a neutral solution, an initial peak at 4.6 V was observed after 3 s and a second peak at 4.4 V after 50 s. This peak was followed by a gradual decrease to 2.5 V after 600 s. In acidic solutions with a pH between 1.5 and 2.5, the initial peak and steady growth potentials occurred at much lower potentials. In a neutral solution, the formed PPy layer was inhomogeneous and relatively rough, and small crater-like features were observed on the surface of the black PPy layer. It is

likely that oxygen gas bubbles were evolved because of the relatively positive polymerisation potential; however, vigorous evolution of oxygen bubbles was not observed.

Figure 2 shows the effect that the mixture ratio has in the acidic pH range between pH 4 and 2 during constant current polymerisation at 3.0 mA cm^{-2}. The transient potential was similar to that observed in acidic solutions, as shown in Figure 1. The initial peak potential was dependent on the pH of the solution; the peak potential was approximately 3.7 V in the solution containing a 20:80 tartaric acid:sodium tartrate mixture (pH 4.0) and was approximately 1.8 V in the solution containing a 94:6 tartaric acid:sodium tartrate mixture (pH 2.0). The potential during the subsequent constant polymer growth also decreased with a decrease in pH.

In an acidic solution with a pH lower than 2.5, high anodic dissolution prevented the potential from increasing sufficiently to polymerise Py when a current density (CD) smaller than 3 mA cm^{-2} was applied. To initiate polymerisation, a potential of at least 0.8 V vs. SSE was required in the acidic tartrate solution. For example, when a CD of 1.0 mA cm^{-2} was applied to the coated steel in a 0.5 M tartaric acid solution at pH 1.5, the potential initially increased to a maximum of 0.4 V. After this initial increase, the potential immediately decreased to −0.78 V, and a PPy layer was not observed on the alloy surface after 600 s of oxidation. Table 1 shows the effect of the mixture ratio of 0.5 M tartaric acid and 0.5 M sodium tartrate

and CD on the formation of PPy films. In an acidic solution at pH 2.0, only CD higher than 3 mA cm^{-2} could form a PPy layer. In a solution with a pH larger than 4, the PPy layer was successfully formed with a low CD of 1 mA cm^{-2}. However, for the PPy layer formed in the solution with larger pH values, small cracks in the film expanded during drying in a desiccator. Potentially, the PPy layers formed in the neutral solutions did not adhere sufficiently to the substrate, and shrinkage during drying induced the formation of these small cracks. Compact and adhesive PPy layers could be prepared in solutions with a pH smaller than 4. When the potential during PPy polymerisation exceeded 2 V, oxygen evolution potentially occurred, and therefore, lower potentials during PPy polymerisation may be preferable. In this paper, we selected an acidic mixture of 0.5 M tartaric acid and 0.5 M sodium tartrate with a molar ratio of 92:8 at pH 2.1 as the optimal acidic solution for the preparation of a compact and adhesive PPy layer on the alloy surface. The acidic tartrate solution at pH 2.1 was used for the preparation of PPy layers in the following sections unless otherwise noted.

When Py was polymerised at lower CD, a denser and more homogeneous PPy layer was formed. This will be described in the following section using SEM characterisation. In the acidic solution at pH 2.1, we utilised an optimised two-step polymerisation; in the first step, we applied a relatively large CD of 5 mA cm^{-2} for 100 s, which can both overcome the active dissolution of the 55% Al–Zn coating and initiate the polymerisation of PPy.

In the second step, the relatively small CD of 1 mA cm^{-2} was applied for 2500 s to obtain a dense PPy layer. The total charge used for the preparation of the PPy layer was usually 3.0 C cm^{-2}.

3.2 Surface morphology and depth profile of PPy layer formed in a tartrate solution

The surface morphology of the PPy layer was found to be dependent on the applied CD. Figure 3 shows the SEM image of the PPy layers formed by single step polymerisation at 5 mA cm^{-2} for 600 s (A) and by the two-step polymerisation (B). The PPy layer consisted of agglomerated cylindroids on which small spherical protuberances grew. In Figure 3, the size of the cylindroids in the PPy layer formed by the single step was shown to be slightly larger than those formed by the two-step polymerisation.

The depth profile of the PPy layer was measured by GD-OES. The result is shown in Figure 4, where the depth profiles of the elements C, H, N, O, Al, and Zn are plotted against sputtering time. Because Al and Zn were not observed between the initial sputtering time and 170 s, it was determined that Al and Zn in the substrate did not penetrate into the PPy layer.

3.3 Addition of molybdate anions to the PPy doped with tartrate anions

Molybdate anions are known to work as an efficient corrosion inhibitor of zinc and its alloys [35, 36], and these anions are expected to stabilise the

passive film. When molybdate is doped into a PPy layer, an improvement of the corrosion protection of 55% Al–Zn-coated steels is expected. The doping of molybdate into a PPy layer was reported by Paliwoda-Porebska *et al.* [8].

For the formation of the PPy layer, we added sodium molybdate with a 5.0 mM concentration to the acid tartrate solution. In our previous work [34], the addition of high concentrations of molybdate to the Py monomer solution prevented the formation of PPy and resulted in the formation of a black salt layer of zinc molybdate. In this study, therefore, we chose the low molybdate concentration of 5.0 mM. Figure 5 shows the potential change during the two-step electropolymerisation in the acidic tartrate solution at pH 2.1 both with and without sodium molybdate. In Figure 5, molybdate addition decreases the polymerisation potential by approximately 0.3 V at the initial CD of 5 mA cm^{-2} and by 0.1–0.2 V during the second step at a CD of 1 mA cm^{-2}, when compared with the solution without molybdate.

The addition of molybdate changed the surface morphology of the PPy layer. Figure 6 shows the SEM image of surface of the PPy layer. When compared with the surface image in Figure 3, the surface particles of the PPy layer formed in the solution containing molybdate are smaller, with diameters of approximately 5 μm.

Doping of the PPy layer by molybdate anions was confirmed by GD-OES depth analysis. This result is shown in Figure 7 and indicates that a detectable amount of molybdate is incorporated in the PPy layer.

3.4 Optical characterisation of PPy layer

The deposition of the polymerised PPy on 55% Al-Zn-coated steel was confirmed by infrared reflection absorption spectroscopy (IR-RAS) and Raman spectroscopy (RS). The IR-RAS and RS spectra are shown in Figure 8 for the PPy layer formed by two-step polymerisation in the acidic tartrate solution with or without sodium molybdate. For the measurement of IR-RAS, the reflectance (R) from the PPy layer on 55% Al-Zn-coated steel was normalised to the reflectance (R_0) of the 55% Al–Zn-coated steel without a PPy layer and converted to an absorbance value.

$$\text{Absorbance} = -\log (R/R_0)$$

The absorption peaks in the IR-RAS and the peaks in the RS were in agreement with those previously reported for PPy [37–45]. Although there were small differences in wavenumber between the IR–RAS peaks described in this report and the ordinary absorption peaks reported with a transmission absorption technique, the absorption peaks at 1525, 1439, 1288, and 1162 cm^{-1} could be, respectively, assigned to C=C backbone stretching, C–C ring stretching, C–N ring stretching, and C–C stretching [37–40]. In the small wavenumber region, the absorption at 1031 cm^{-1} may correspond to N–H in-plane deformation, and the absorption at 953 cm^{-1} may correspond to C–H out-of-plane vibration [37-40]. The Raman bands were also related to those of PPy as follows: C=C backbone stretching at 1587 cm^{-1}, N–C ring

stretching and C–C ring stretching at 1425 cm^{-1}, C–C stretching at 1324 cm^{-1}, C–H in-plane bending at 1042 cm^{-1}, and ring deformation at 985 cm^{-1} [41–45].

As shown in Figure 8, the spectra of the PPy layers formed in solutions containing molybdate were almost identical to those of the PPy layer formed without molybdate, and the presence of molybdate did not influence the formation of PPy, except for the observed decrease in potential during constant current polymerisation.

3.4 Thickness of PPy Layer

Confocal laser scanning optical microscopy was used to measure the thickness of the PPy layers formed under various conditions to assess the quantitative relationship between the layer thickness and the anodic charge passed.

Figure 9 shows the estimated thickness as a function of anodic charge passed. Figure 9 shows data for PPy layers that were formed in three solutions by the two-step polymerisation in which 5 mA cm^{-2} was first applied for 100 s and 1 mA cm^{-2} was then applied for various time periods. The PPy layer thickness was found to increase with a rate of 3.7 μm $(C\ cm^{-2})^{-1}$ in the acidic tartrate solution at pH 2.1, and the thickness was not influenced by the addition of molybdate into the solution. However, the PPy layer grew with a rate of 4.6 μm $(C\ cm^{-2})^{-1}$ in the tartaric acid solution. When

these results were compared with the values reported in our previous paper on steel covered with a PPy layer doped with phospho-molybdate heteropolyanions ($PMo_{12}O_{40}^{3-}$) [46], the ratio of thickness to charge passed was 1.3–1.6 times larger than for the layer doped with $PMo_{12}O_{40}^{3-}$. This difference may be because of a change in volume of the doped anions and the doping ratio.

By utilising the linear relationship shown in Figure 9 between the thickness of the PPy layer and the charge passed for polymerisation, the thickness of the PPy layer can be controlled by CD and the time period of constant current polymerisation. This is the case even though there is not enough evidence for the charge efficiency of the PPy polymerisation. Potentials more positive than 1.2 V during polymerisation, as shown in Figures 1, 2, and 5, indicated that oxygen gas evolution possibly occurred; however, because we did observed any gas bubbles on the surface, it is possible that the charge efficiency for the PPy polymerisation was close to 100 %.

3.5 AC impedance under dry conditions

To assess the conductive properties of the PPy layer and the dielectric properties of the passivating interfacial oxide film, we measured the AC electric response of the PPy layer covering the 55% Al–Zn-alloy-coated steel under dry conditions after polymerisation. The measured AC impedance

reflects the electronic properties of the PPy layer and the interfacial oxide film.

The AC impedance response of the 55% Al–Zn-coated steel covered with the PPy layer is shown in Figure 10, where the real part is plotted against the imaginary part (the Nyquist plot). From the semicircle in Figure 10, the equivalent circuit shown in Figure 11 was assumed, which consists of a series connection of a resistance R_{PPy} of the conducting PPy layer with a parallel R_{ox}-C_{ox} circuit for the dielectric interfacial thin oxide layer. We found the same layer structure illustrated in Figure 12 in a previous paper concerning a PPy layer formed on a zinc electrode in a tartrate solution [34].

Using the Nyquist plot, the electrical elements of the equivalent circuit can be estimated. From the values of Real(Z) at the high frequency limit and the low frequency limit, one can respectively evaluate R_{PPy} and R_{ox}. From the frequency (f_0) at the top of the semicircle, the time constant (τ) of the parallel circuit can be evaluated, and C_{ox} can be estimated using τ and R_{ox}.

$$C_{ox} = \tau / R_{ox} = 1/(2\pi f_0 R_{ox})$$

The evaluated results are listed in Table 2 as well as the thickness of the interfacial thin oxide film, which was estimated from the capacitance assuming that the dielectric constant of the oxide film is ε = 9.84. This dielectric constant value is the value for the anodic oxide film of aluminium [47]. The thickness of the interfacial oxide layer ranged from 10 to 15 nm.

The impedance was affected by the addition of sodium molybdate. As

shown in Figure 10 and Table 2, the resistance (R_{ox}) of the interfacial oxide film formed on the Al–Zn alloy in the solution containing molybdate is 4 to 5 times larger than that in the solution without molybdate. Additionally, the resistance of the PPy layer (R_{PPy}) became smaller when molybdate was added. Consequently, the addition of molybdate produced a more conductive PPy layer and a more insulating oxide film.

3.6 Corrosion test in a 3.5 wt% NaCl solution

The corrosion protection of the PPy layer was tested by immersion of the steel sample in a 3.5 wt% NaCl solution. During immersion, the open circuit potential (OCP) or corrosion potential was traced, and the surface of the PPy coated steel was checked for the appearance of corrosion products. The OCP is plotted in Figure 12 for the coated steels covered by a PPy layer formed under three current conditions in the acidic tartrate solution with a pH of 2.1. In Figure 12, the OCP of a bare 55% Al–Zn-coated steel without PPy was also plotted as a comparison. The conditions for the electropolymerisation of the three samples were as follows: (1) 5 mA cm^{-2} for 600 s with a total charge of 3 C cm^{-2} and a thickness of 11 μm, (2) initially, 5 mA cm^{-2} for 100 s and subsequently 1 mA cm^{-2} for 2500 s with a total charge of 3 C cm^{-2} and a thickness of 11 μm, and (3) initially, 5 mA cm^{-2} for 100 s and subsequently, 1 mA cm^{-2} for 4500 s with a total charge of 5 C cm^{-2} and a thickness of 19 μm. The potential of the PPy layer covering the 55% Al–Zn-coated steel initially

exhibited high values from 0 to −0.4 V, which corresponds to the passive state of the 55% Al–Zn alloy, and the potential subsequently gradually reduced to an active state potential between −0.96 and −1.03 V. On the contrary, uncoated 55% Al–Zn-coated steel had an active potential of −1.05 V vs. SSE when initially immersed in 3.5 wt% NaCl. When the potential was more positive than −0.7 V, no corrosion products were observed on the black PPy layer. However, while in the active state at approximately −1 V, a white corrosion product immediately appeared on the surface. The length of time necessary for the potential to decay to −0.7 V may be an indicator of corrosion protection efficiency. As shown in Figure 12, the PPy layer formed by the two-step polymerisation was found to be more efficient for the PPy layers formed with a total charge of 3 C cm^{-2}. Comparing PPy layers formed with 3 and 5 C cm^{-2} total charge indicates that thicker PPy layers may be more effective at preventing corrosion.

Figure 13 shows the effect of molybdate anion incorporation on the protection of 55% Al–Zn-coated steel against corrosion. As shown in Figure 13, the addition of molybdate increased corrosion protection because the time period necessary for the potential to decrease to −0.7 V was approximately 60 h, ten times larger than the corresponding time period observed for the PPy layer formed without molybdate.

3.7 Electrochemistry of 55% Al–Zn-coated steel coated with PPy layers

To examine the protection mechanism, potential-current curves for 55% Al–Zn-coated steel coated with a PPy layer doped with either tartrate and molybdate ions or only with tartrate ions were measured by the linear potential sweep method using a sweep rate of 5×10^{-3} V s^{-1} in a 3.5% NaCl solution under air after the steel sample was immersed for 30 min in the NaCl solution. The potential range for the potential-current measurement was restricted between (E_{OCP} − 0.20) V and (E_{OCP} + 0.60) V to avoid large changes in the redox property of the PPy layer before the measurement. These results are shown in Figure 14 as well as the potential-current curve of bare 55% Al–Zn-coated steel. The corrosion CD was estimated for bare 55% Al–Zn-coated steel to be 2.9 μA cm^{-2} from extrapolation of the Tafel lines. In the anodic branch, the current of the bare 55% Al–Zn alloy sharply increased to 100 mA cm^{-2} at -0.4 V, and no passive region was observed. The 55% Al–Zn-coated steel covered by PPy layers exhibited larger OCP and larger exchange CDs of 38 μA cm^{-2} and 20 μA cm^{-2} for the coated steels covered by the PPy-tartrate layer and PPy-tartrate-molybdate layer, respectively. Larger OCPs indicate that the PPy layer is acting as an oxidant to the 55% Al–Zn alloy. The high exchange CDs at the OCPs do not correspond to the corrosion CD of the PPy-covered specimens but to redox CD of the oxidative PPy layer,

$$PPy^{x+}\oplus(x/y)A^{y-} + e = PPy^{(x-y)+}\oplus[(x\square y)/y]]A^{y\square} + A^{\square}_{aq}$$

where $A^{\square}_{aq}$ represents an anion removed from the PPy layer into the aqueous

solution. The redox potential of the PPy layer is determined by the oxidation degree, x, which gradually decreases with an increase in immersion time. The oxidation degree eventually reaches x = 0, which corresponds to neutral PPy. The anodic CD of the 55% Al–Zn-coated steel covered by the PPy layers shown in Figure 15 remains much smaller than that of the bare 55% Al–Zn. The current was assumed to be an oxidation current of the PPy layer. The anodic CD of the 55% Al-Zn-coated steel covered by the PPy-tartrate layer displayed a sharp increase from 0.32 V ((a) in Figure 14). This increase may correspond to an initiation of pitting corrosion for the Al-Zn-coating layer. For the coated steel covered by the PPy-tartrate-molybdate layer, no similar increase of anodic CD was observed ((b) in Figure 14).

The electrochemical impedance spectroscopy (EIS) was also measured during immersion in a 3.5% NaCl solution. Figure 15 shows Nyquist plots of the impedance for 55% Al–Zn-coated steel covered by a 11 μm thick PPy-tartrate-molybdate layer, which was formed by the two-step method. The response shown in Figure 15(a), which was measured after 0.5 h of immersion, probably consisted of two semicircles. However, the semicircle between 5 Hz and 10 mHz was not completed. The diameter of the semicircle at higher frequencies increased with an increase in the immersion time, as shown in Figure 15. The low-frequency semicircle decreased in intensity with longer immersion periods and had almost disappeared after 19.9 h of immersion.

For the impedance response, we assumed an equivalent circuit shown in Figure 16 in which the equivalent circuit consisted of two parallel R-C circuits connected in series, and the R-C circuit in the lower frequency region potentially includes the Warburg diffusion impedance. We believe that the parallel R_{it}-C_{dl} circuit at higher frequencies corresponds to the electrochemical response at the interface between the PPy layer and the solution, and R_{it} and C_{dl} were respectively an ionic transfer resistance at the interface and a double layer capacitance. The second parallel circuit in the lower frequencies may correspond to ionic transfer and diffusion elements in the PPy layer [47, 48]. $R_{i\text{-}PPy}$ was assumed to be an ionic transfer resistance through the PPy layer, W is the Warburg diffusion impedance of mobile ions in the PPy layer, and C_{redox} is the redox capacitance of the PPy layer [48, 49]. The circuit of $(R_{i\text{-}PPy}-W)-C_{redox}$ at lower frequencies, however, was not examined in further detail because the semicircle was not completed in the frequency range applied to this study. In the latter section, we examine only the semicircle in the higher frequency region.

The EIS responses of the 55% Al–Zn alloy covered by the PPy-tartrate layer is shown in Figure 17 in which the EIS was measured after immersion in the 3.5% NaCl solution for 0.5 h and 4.8 h. From the diameter of the semicircle at higher frequencies and the specific frequency (f_0) at the top of the semicircle in Figures 15 and 17, one can simulate the values of R_{sol}, R_{it}, and C_{dl}. The simulated values are listed in Table 3. The simulation was

performed in a similar manner to that of the previous AC impedance spectroscopy measured under dry conditions. The ion transfer resistances R_{it} at the PPy-solution interface slightly increased with the immersion time and were 2 to 3 times larger for the specimen covered by the PPy-tartrate-molybdate layer than for the sample covered by the PPy-tartrate layer. The increase of R_{it} indicates that the ion exchange rate between the PPy layer and solution is decreased with degradation of the PPy layer, and the rate for the PPy layer containing molybdate ions is smaller than that of the layer without molybdate. The simulated double layer capacitance, C_{dl}, for the specimen covered by the PPy-tartrate-molybdate layer was smaller than the capacitance for the PPy-tartrate layer, and the capacitances were smaller than the usual double layer capacitance of metal electrodes. The cause of the small capacitance value has not been elucidated. We hypothesise that the inner oxide layer partially contributes to the capacitance value.

The PPy layer lost its oxidant property after long periods of immersion in the NaCl solution and could not maintain the passive state of 55% Al–Zn-alloy coating. The OCP of the alloy coating covered by the less oxidative PPy layer reached a potential of approximately −1.0 V, which corresponds to that of bare 55% Al–Zn alloy. The PPy layer after long immersions may be changed to a neutral form. Figure 18 shows the impedance response of the 55% Al–Zn-alloy-coated steel covered by a neutral

PPy layer immersed for long time period. The semicircle was suppressed, and the diameter became smaller (150-160 $\Omega\,cm^2$) when compared with the results of the oxidative PPy shown in Figures 15 and 17.

4. Discussion

4.1 Structure of the PPy layer electropolymerised on a 55% Al–Zn-alloy coating

Figure 19 shows the initial transient of potentials under constant current control at 3 mA cm^{-2} in the acidic tartrate solutions. The results in Figure 19 correspond to the potential change in the initial 35 s shown in Figure 2. During oxidation under constant current control, the potential linearly increased from the initial immersion potential of −1.4 V to 2 V in 2 s, and the potential peaked at a maximum of 2.5–3.0 V within 5 s. In the initial period of 5 s, an oxide film is assumed to grow, and the nucleation of PPy began. After the initial 5 s, the three-dimensional growth of the PPy layer was initiated. The layer formed on the 55% Al–Zn alloy is, therefore, assumed to consist of a bi-layer of a thin insulating inner oxide layer and an outer conducting PPy layer. In a previous study on a PPy coated zinc electrode, we observed by SEM an interfacial oxide/salt layer between the zinc substrate and the PPy layer in a cross-sectional view of the sample [34]. Because the interfacial oxide layer on the 55% Al–Zn alloy was assumed

to be much thinner than that found on the zinc electrode, it might be difficult to observe the oxide layer in cross section using SEM.

The formed inner layer is assumed to work as a dielectric layer that induces a semicircle on the complex plane plot of the impedance under dry conditions, as shown in Figure 10. The thin and insulating oxide is also assumed to work as a passivation barrier against corrosion. The outer conducting PPy layer has oxidative properties that can help to maintain the inner passive oxide.

The outer PPy layer has conductive properties. Using the thickness (d) of 11 μm shown in Figure 9 and the resistance of the PPy layer listed in Table 2, the conductance (σ) of the PPy layer can be estimated. Using the equation,

$$\sigma = d / R_{PPY}$$

the conductance of the PPy layer formed in the pH 2.1 solution of tartaric acid and sodium tartrate was estimated to be $3–10\times10^{-5}$ Ω^{-1} cm^{-1}, and the conductance in the solution containing molybdate was estimated to be 2×10^{-4} Ω^{-1} cm^{-1}. Because the measured resistance includes a contribution of a contact resistance between the gold disc and the PPy layer, the exact conductance of the PPy layer may be larger than the calculated value.

4.2 Effect of solution pH on PPy formation on 55% Al–Zn coating

The potential transient during the constant current oxidation is very dependent on the pH of the mixture of tartaric acid and sodium tartrate as

shown in Figures 1, 2, and 19. As shown in Figures 2 and 19, after the initial maximum, the potential decreased over time to a steady potential, at which time three-dimensional growth of the PPy layer occurs. Both the initial maximum and steady potential are lower in the more acidic solution. The polymerisation of Py is assumed to occur with a smaller overvoltage in the more acidic solution.

The model shown in Figure 20 may explain the effect of solution pH on the PPy formation. In a neutral solution, the applied current produces a thick anodic oxide, and electron transfer for PPy formation occurs only through a small density of defect sites, which results in a patch-like inhomogeneous PPy layer. In acidic solutions, the dissolution of the 55% Al–Zn alloy occurs preferentially when a small current is applied and the potential polarised by the current does not reach the polymerisation potential of approximately 0.8 V. When a larger current is applied, growth of the oxide film occurs, and the oxide film's growth is restricted to a small thickness by the film's simultaneous dissolution. The thin oxide may include a relatively large number of defect sites through which electron transfer can occur from the Py monomer in aqueous solution to the Al–Zn-alloy substrate. This electron transfer produces a homogeneous PPy layer.

In alkaline solutions, the growth of the oxide film is expected and may inhibit the PPy polymerisation on the Al–Zn alloy. Saidman et al., however, reported a successful formation of a PPy layer on aluminium by growing the

oxide film in an alkaline solution at pH 12 that contained nitrate and molybdate anions [13-15]. Molybdate anions may play a large role in PPy formation because the molybdate anions enhance the polymerisation of PPy potentially by acting as a catalyst. The catalytic properties of molybdate may be related to the redox properties of Mo(VI) and Mo(V). Addition of molybdate in this study produced a smaller anodic overvoltage during the galvanostatic polymerisation, as shown in Figure 6.

4.3 Effect of current applied on PPy formation and corrosion protection

The current used for the polymerisation of the Py monomer may influence the surface morphology of the PPy layer. The morphology of the PPy layer consisted of agglomerated small cylindroids, the size of which depended on the applied current. A smaller current produced smaller cylindroids and, therefore, smaller crevices or channels between the cylindroids. This may be the origin of the increased protective properties of the PPy layer when it is formed at lower current.

To form a dense and compact PPy layer, we utilised the two-step polymerisation method. This method uses an initial polymerisation with a large current of 5 mA m^{-2} to overcome the initial dissolution and to initiate nucleation of PPy. A second polymerisation is then utilised with a smaller current of 1 mA cm^{-2} for growth of a dense and compact PPy layer composed of fine particles. The PPy layer formed by the two-step polymerisation

method displayed relatively high corrosion protection of the Al–Zn alloy, as shown in Figure 12.

4.4 Model of corrosion protection by oxidative and conducting PPy

The redox potential of the oxidative PPy layer formed is significantly more positive than that of the corrosion potential of the bare 55% Al–Zn-alloy-coated steel, as shown in Figure 14. Because the exchange redox current of the PPy at the OCP is much larger than that of the corrosion current of the bare 55% Al–Zn-alloy-coated steel, the potential of the 55% Al–Zn alloy with the PPy layer can be shifted to the redox potential of the PPy layer. Without the PPy layer, the anodic current of 55% Al–Zn alloy sharply increases to 100 mA cm^{-2} with an increase in potential and no passivation was observed. Potentially, active dissolution of the 55% Al–Zn alloy is followed by pitting corrosion as a result of chloride attack. The PPy layer covering the 55% Al–Zn-alloy coating shifts the potential to more positive values. This shift facilitates the formation of a passive oxide on the 55% Al–Zn alloy and allows the oxide to be stably maintained. Although the composition of the passive oxide was not analysed in this study, the passive film potentially includes tartrate and/ or molybdate complexes of aluminium and zinc.

4.5 Effect of the addition of molybdate anions into the PPy layer on corrosion

protection

Molybdate anions added to the acidic tartrate solution are incorporated in the PPy layer during polymerisation (Figure 7) and change the surface morphology of the PPy layer to an agglomerate of fine granules (Figure 6). Further ion exchange between the PPy layer and solution was suppressed, as shown in Figure 15 and 17.

Molybdate anions may themselves act as a corrosion inhibitor of the passivated Al–Zn alloy [35, 36], and molybdate anions can induce the formation of a more stabilised passivation film on the 55% Al–Zn-alloy coating. Because molybdate anions can be stored in the PPy layer as dopant anions, the anion's inhibitive effect continues for a relatively long time period. When the PPy layer and the passive oxide are locally destroyed, molybdate anions released from the PPy potentially repair the damaged passive oxide, and the passive state of 55% Al-Zn coating will remain [8, 9]. In addition to the inhibitive effect, molybdate anions allow for the formation of a finer and denser PPy layer. Both effects can induce a longer duration of passivation during immersion in a sodium chloride solution, as shown in Figure 13.

5. Conclusion

For corrosion protection, a polypyrrole (PPy) layer was formed on 55% Al–Zn-coated steel.

(1) A dense layer of PPy was successfully formed in an acidic tartrate solution at pH 2.1. The film potentially consists of an inner thin layer of zinc and/or aluminium oxide and an outer PPy layer doped with tartrate anions.

(2) The PPy layer can passivate 55% Al–Zn-coated steel in a 3.5 wt% aqueous NaCl solution for several hours.

(3) Doping of molybdate anions into the PPy-tartrate film significantly improved the film's protective properties. Doping of molybdate anions produced a denser PPy layer, and the rate of anion exchange between the PPy layer and solution was decreased. The PPy-tartrate-molybdate layer, therefore, improved the duration of passivation of 55% Al–Zn-coated steel in a 3.5 wt% NaCl solution to 60 hours, during which time no appreciable corrosion was observed.

References

[1] D. E. Tallman, G. Spinks, A. Dominis, G. G. Wallace, J. Sol. State Electrochem., 6 (2002) 73–84.

[2] M.B. González, S.B. Saidman, Corros. Sci., 53 (2011) 276–282.

[3] W. Qafsaoui, H. Takenouti, Corros. Sci,. 52, (2010) 3667–3676.

[4] M.E. Nicho, V.M. Salinas-Bravo, J.G. Chacon-Nava, A. Martinez-Villafañe, Corros. Sci., 52 (2010) 1086–1092.

[5] D.O. Flamini, S.B. Saidman, Corros. Sci., 52 (2010) 229–234.

[6] N.D. Nam, J.G. Kim, Y.J. Lee, Y.K. Son, Corros. Sci., 51 (2009) 3007–3013.

[7] J. H. W. deWit, Inorganic and Organic Coating, in: P. Marcus and J. Oudur (Eds.), Corrosion Mechanism in Theory and Practice, Marcel Dekker, New York,1995, pp. 613–614.

[8] G. Paliwoda-Porebska, M. Rohwerder, M. Stratmann, U. Rammelt, Le Minh Duc, W. Plieth, J. Sol. State Electrochem., 10 (2006) 730–736.

[9] D. Kowalski, M. Ueda, T. Ohtsuka, J. Mater. Chem., 20 (2010) 7630–7633.

[10] S. B. Saidman, J. B. Bessone, J. Electroanal. Chem., 521 (2002) 87–94.

[11] G. S. Akundy, J. O. Iroh, Polymer, 42 (2001) 9665–9669.

[12] L. Makhloufi, H. Hammache, B. Saidani, Electrochem. Comm., 2 (2000) 552-556.

[13] I. L. Lehr, S. B. Saidman, Electrochim. Acta, 51 (2006) 3249-3255.

[14] S. B. Saidman, J. Electroanal. Chem., 534 (2002) 39–45.

[15] S. B. Saidman, O. V. Quinzani, Electrochim. Acta, 50 (2004) 127–134.

[16] M. Barzzaoui, J. I. Martins, T. C. Reis, E. A. Bazzaoui, M. C. Nunes, L. Martins, Thin Solid Films, 485 (2005) 155–159.

[17] M. Barzzaoui, J. I. Martins, S. C. Costa, E. A. Bazzaoui, T. C. Reis, l. Martins, Electrochim. Acta, 51 (2006) 2417–2426.

[18] J. I. Martins, S. C. Costa, M. Bazzaoui, G. Goncalves, E. Fortunato, R. Martins, J. Power Sources, 160 (2006) 1471–1479.

[19] I. L. Lehr, S. B. Saidman, Mater. Chem. and Phys., 100 (2006) 262–267.

[20] S. D. Saidman, M. E. Vela, Thin Solid Films, 493 (2005) 96–103.

[21] M.-L. Tsai, J. Power Sources, 173 (2007) 613–620.

[22] J. I. Martins, S. C. Costa, M. Bazzaoui, G. Goncalves, E. Fortunato, R. Martins, Electrochim. Acta, 51 (2006) 5802–5810.

[23] K. Naoi, M. Takeda, H. Kanno, M. Sakakura, A. Shimada, Electrochim. Acta, 45 (2000) 3413–3421.

[24] J. Petitjean, S. Aeiyach, J. C. lacroix, P. C. Lacaze, J. Electroanal. Chem., 478 (1999) 92–100.

[25] J. Petitjean, J. Tanguy, J. C. Lacroix, K. I. Chanw-Ching, S. Aeiyach, M. Delamar, P. C. Lacaze, J. Electroanal. Chem., 581(2005) 111–121.

[26] B. Zaid, S. Aeiyach, P. C. Lacaze, H. Takenouti, Electrochim. Acta, 43, (1998) 2331–2339.

[27] S. Aeiyach, B. Zaid, P. C. Lacaze, Electrochim. Acta, 44 (1999) 2889–2898.

[28] J. I. Martins, T. C. Reis, M. Bazzaoui, E. A. Bazzaoui, R. Martins, Corros. Sci., 46 (2004) 2361–2381.

[29] M. Bazzaoui, L. Martins, E. A. Bazzaoui, J. I. Martins, J. Electroanal. Chem., 537 (2007) 47–57.

[30] J. Vatsalarani, S. Geetha, D. C. Trivedi, P. C. Warrier, J. Power Sources, 158 (2006) 1484–1489.

[31] M. H. Pournaghi-Azar, H. Nahalparvari, Electrochim. Acta, 50 (2005)

2107−2115.

[32] B. Zaid, S. Aeiyach, P. C. lacaze, Synth. Met., 65 (1994) 27−34.

[33] M. Bazzaoui, E. A. Bazzaoui, L. Martins, J. I. Martins, Synth. Met., 128 (2004) 103−114.

[34] S. Tsuchiya, M. Ueda, T. Ohtsuka, ISIJ International, 47, (2007) 151−156.

[35] E. Almeida, T. C. Diamantino M. O. Figueiredo, Carlos Sá, Surf. and Coat. Techn., 106 (1998) 8−17.

[36] A.A.O. Magalhães, I.C.P. Margarit, O.R. Mattos, J. Electroanal. Chem., 572 (2004) 433−440.

[37] J. C. Iroh, G. A. Wood, Composites B, 298 (1998) 181−188.

[38] M. Bazzaoui, L. Matins, E. A. Bazzaoui, J. I. Martins, Electrochim. Acta, 47 (2002) 2953−2962.

[39] R. M. G. Rajapakse, R. M. M. Y. Rajapakse, H. M. N. Bandara, B. S. B. Karunarathue, Electrochim. Acta, 53 (2008) 2946−2952.

[40] R. M. G. Rajapakse, K. Murakami, H. M. N. Bandara, R. M. M. Y. Rajapakse, Electrochim. Acta, 55 (2010) 2490−2497.

[41] K. Furukawa, S. Tazawa, Y. Fujii, I. Harada, Synth. Met., 24 (1988) 329−341.

[42] J. Bukowska, K. Jackowska, Synth. Met., 35 (1990) 143−150.

[43] T. Ohtsuka, T. Wakabayashi, H. Einaga, Synth. Met., 79 (1996) 235−239.

[44] K. Crowley, J. Cassidy, J. Electroanal. Chem., 547 (2009) 75−82.

[45] H. Nguyen Thi Le, M. C. Bernard, B. Garcia-Renaud, C. Deslouis, Synth. Met., 140 (2004) 287−293.

[46] T. Ohtsuka, M. Iida, M. Ueda, J. Sol. State Electrochem., 10 (2006) 714−720.

[47] K. Watanabe, M. Sakairi, H. Takahashi, K. Takahiro, S. Nagata, S. Hirai, J. Electrochem. Soc., 148 (2001) B473−B481.

[48] R. D. Armstrong, J. Electroanal. Chem., 198 (1986) 177−180.

[49] C. E. D. Chidsey, R. W. Murray, J. Phys. Chem., 90 (1986) 1479-1984.

Captions

Table 1 The formation of PPy layers in mixtures of 0.5 M tartaric acid and 0.5 M sodium tartrate at various pH values.

Table 2 Resistance of the PPy layer, R_{PPY}, resistance of the interfacial oxide layer, R_{ox}, and capacitance the interfacial oxide layer, C_{ox}. The thickness, d, of the oxide layer was determined using C_{ox}.

Table 3 Values for the electric elements of the equivalent circuit for 55% Al-Zn-coated steel covered by the PPy-tartrate-molybdate or the PPy-tartrate layer during immersion in a 3.5% NaCl solution where R_{it} is the ion transfer resistance, C_{dl} is the double layer capacitance, and R_{sol} is the solution resistance.

Fig. 1 Potential transient during the polymerisation of polypyrrole (PPy) at current density (CD) of 5 mA cm^{-2} in a solution of 0.5 M sodium tartrate (pH 8.4) (a), in a 0.5 M tartaric acid solution (pH 1.5) (b), and in a mixture of 0.5 M sodium tartrate and 0.5 M tartaric acid (pH 2.1) (c). The concentration of pyrrole (Py) monomer in the solutions was 0.6 M.

Fig. 2 Potential transients during the polymerisation of PPy at a CD of 3 mA

cm^{-2} in solutions containing various ratios of 0.5 M tartaric acid and 0.5 M sodium tartrate. The molar ratios of tartaric acid to sodium tartrate were (a) 20:80 at pH 4.0, (b) 90:10 at pH 2.5, (c) 92:8 at pH 2.1, and (d) 94:6 at pH 2.0.

Fig. 3 SEM images of the PPy surface on Al–Zn-coated steel. The PPy layer was formed in the acidic tartrate solution at pH 2.1 by (A) constant current oxidation at 5 mA cm^{-2} for 600 s and (B) by a two-step oxidation performed initially at 5 mA cm^{-2} for 100 s and subsequently at 1 mA cm^{-2} for 2500 s.

Fig. 4 The elemental depth profile measured by GD-OES for a PPy layer formed on a 55% Al–Zn coating. The PPy layer was formed in the acidic tartrate solution at pH 2.1 by the two-step oxidation process.

Fig. 5 Potential transient during the two-step oxidation in the acidic tartrate solution at pH 2.1 with or without 5 mM of sodium molybdate.

Fig. 6 SEM images of the PPy surface on 55% Al–Zn-alloy-coated steel. The PPy layer was formed by the two-step oxidation process in the acidic tartrate solution at pH 2.1 that contained 5 mM of sodium molybdate.

Fig. 7 The elemental depth profile measured by GD-OES for a PPy layer formed on a 55% Al–Zn coating. The PPy layer was formed by the two-step

oxidation in the acidic tartrate solution at pH 2.1 that contained 5 mM of sodium molybdate.

Fig. 8 (A) IR-RAS spectra and (B) Raman spectra of the PPy layer on 55% Al–Zn-coated steel. The PPy layer was formed using the two-step oxidation process in the acidic tartrate solution at pH 2.1 that contained 5 mM of sodium molybdate.

Fig. 9 The ratio of PPy layer thickness to electric charge passed for a preparation in tartaric acid (pH 1.5) and in the acidic mixture solution of tartric acid-sodium tartrate (pH 2.1) with and without 5 mM sodium molybdate. The polymerisation was performed using the two-step oxidation process where 5 mA cm^{-2} for 100 s was used, followed by 1 mA cm^{-2} for different time periods ranging between 1000 and 9500 s.

Fig. 10 Complex plane plots of impedance for PPy layers on 55% Al–Zn-coated steel. The PPy layer was formed either in the acidic tartrate solution using 5 mA cm^{-2} for 600 s (a), by the two-step oxidation (b), and in the solution containing 5 mM sodium molybdate by the two-step oxidation (c). The frequencies noted in the figure represent characteristic frequencies from the top of the individual semicircles.

Fig. 11 A schematic model of the interfacial phase of the 55% Al–Zn alloy/passive oxide/conductive PPy layer and the corresponding equivalent circuit.

Fig. 12 The open circuit potential (OCP) of 55% Al–Zn-coated steel covered by PPy layers in 3.5 wt% sodium chloride solution. The PPy layers were formed in the acidic tartrate solution by oxidation at 5 mA cm^{-2} for 600 s (a), by the two-step oxidation at 5 mA cm^{-2} for 100 s followed by 1 mA cm^{-2} for 2500 s (b), and by 5 mA cm^{-2} for 100 s followed by 1 mA cm^{-2} for 9000 s (c). The OCP of bare 55% Al–Zn-coated steel was plotted as a comparison.

Fig. 13 The OCP of 55% Al–Zn-coated steel covered by PPy layers in 3.5 wt% sodium chloride solution. The PPy layers were formed in the acidic tartrate solution (a) with and (b) without 5 mM sodium molybdate using the two-step oxidation process.

Fig. 14 Potential-current relationships for 55% Al–Zn alloy coated steel covered with the PPy-tartrate layer (a) or by the PPy-tartrate-molybdate layer (b) in a 3.5% NaCl solution under an air-opened condition. The relationship of uncoated 55% Al–Zn-alloy-coated steel (c) is plotted for comparison. The relationship was measured by the potential sweep method from E_{OCP} − 0.20 V to E_{OCP} + 0.60 V at a sweep rate of 5 mV s^{-1}.

Fig. 15 Nyquist plots of EIS for the 55% Al–Zn-alloy-coated steel covered by the PPy-tartrate-molybdate layer in a 3.5% NaCl solution after immersion for 0.5 h (a), 8.25 h (b1), and 19.9 h (b2) under an air-opened condition. The PPy layers were formed using the two-step oxidation process in the acidic tartrate solution at pH 2.1 that contained 5 mM of sodium molybdate.

Fig. 16 The equivalent circuit of EIS where: R_{sol} is the solution resistance; R_{it} is the ion transfer resistance at the PPy/ solution interface; C_{dl} is the double layer capacitance; $R_{i\text{-}PPy}$ is the ion-transfer resistant in the PPy layer; C_{redox} is the redox capacitance of the PPy layer; and W is the Warburg impedance of ion diffusion in the PPy layer.

Fig. 17 Nyquist plots for the EIS of 55% Al–Zn-alloy-coated steel covered by the PPy-tartrate layer in a 3.5% NaCl solution after immersion for 0.5 h (a) and 4.8 h (b) under an air-opened condition.

Fig. 18 Nyquist plots of EIS for the 55% Al–Zn-alloy-coated steel covered by the PPy-tartrate layer (a) and by the PPy-tartrate-molybdate layer (b) in a 3.5% NaCl solution after immersion for 60 h under an air-opened condition.

Fig. 19 Potential transient in the initial 40 s during polarisation at a CD of 3

mA cm^{-2} in the acidic mixtures of tartaric acid-sodium tartrate at pH 2.1, 2.4, and 4.0. The data correspond to the initial part of Fig. 2.

Fig. 20 A schematic model for the formation of a PPy layer on 55% Al–Zn in neutral and acidic solutions.

Table 1 The formation of PPy layers in mixtures of 0.5 M tartaric acid and 0.5 M sodium tartrate at various pH values.

Volume ratio of tartric acid to sodium tartrate	20:80	90:10	92:8	94:6
Current Density / mA cm^{-2}	pH 4.0	pH 2.5	pH 2.1	pH 2.0
1	○	×	×	×
2	○	○	○	×
3	○	○	○	○
5	○	○	○	○

○: The PPy can be formed.
×: The potential does not rise to enough high potential to polymerize pyrrole.

Table 2 Resistance of the PPy layer, R_{PPY}, resistance of the interfacial oxide layer, R_{ox}, and capacitance the interfacial oxide layer, C_{ox}. The thickness, d, of the oxide layer was determined using C_{ox}.

Condition of PPy formation			R_{PPr}/ Ω cm^2	R_{ox}/Ω cm^2	C_{ox}/ 10^{-7}F cm^{-2}	d/ nm
i/ mA cm^{-2}	Q/ C cm^{-2}	Solution				
5.0	3.0	Mixture Solution at pH 2.1	36	7.5×10^2	6	15
5.0→1.0	3.0	Mixture Solution at pH 2.1	9.0	6.1×10^2	7	12
5.0→1.0	3.0	Mixture solution at pH 2.1 with 5 mM molybdate	5.0	3.2×10^3	4	23

Table 3 Values for the electric elements of the equivalent circuit for 55% Al-Zn-coated steel covered by the PPy-tartrate-molybdate or the PPy-tartrate layer during immersion in a 3.5% NaCl solution where R_{it} is the ion transfer resistance, C_{dl} is the double layer capacitance, and R_{sol} is the solution resistance.

time	E_{OCP}	R_{it}	C_{dl}	R_{sol}
h	V vs. Ag/ AgCl	Ω cm^2	10^{-6} F cm^{-2}	Ω cm^2
PPy-tartrate-molybdate				
0.5	0.07	750	4.3	3.7
3.7	−0.31	780	4.3	4.4
8.25	−0.13	1020	4.1	4.8
19.9	−0.26	1170	7.2	5.7
PPy-tartrate				
0.5	−0.18	380	13	3.8
1.7	−0.34	380	10	3.4
4.8	−0.75	455	15	4.9

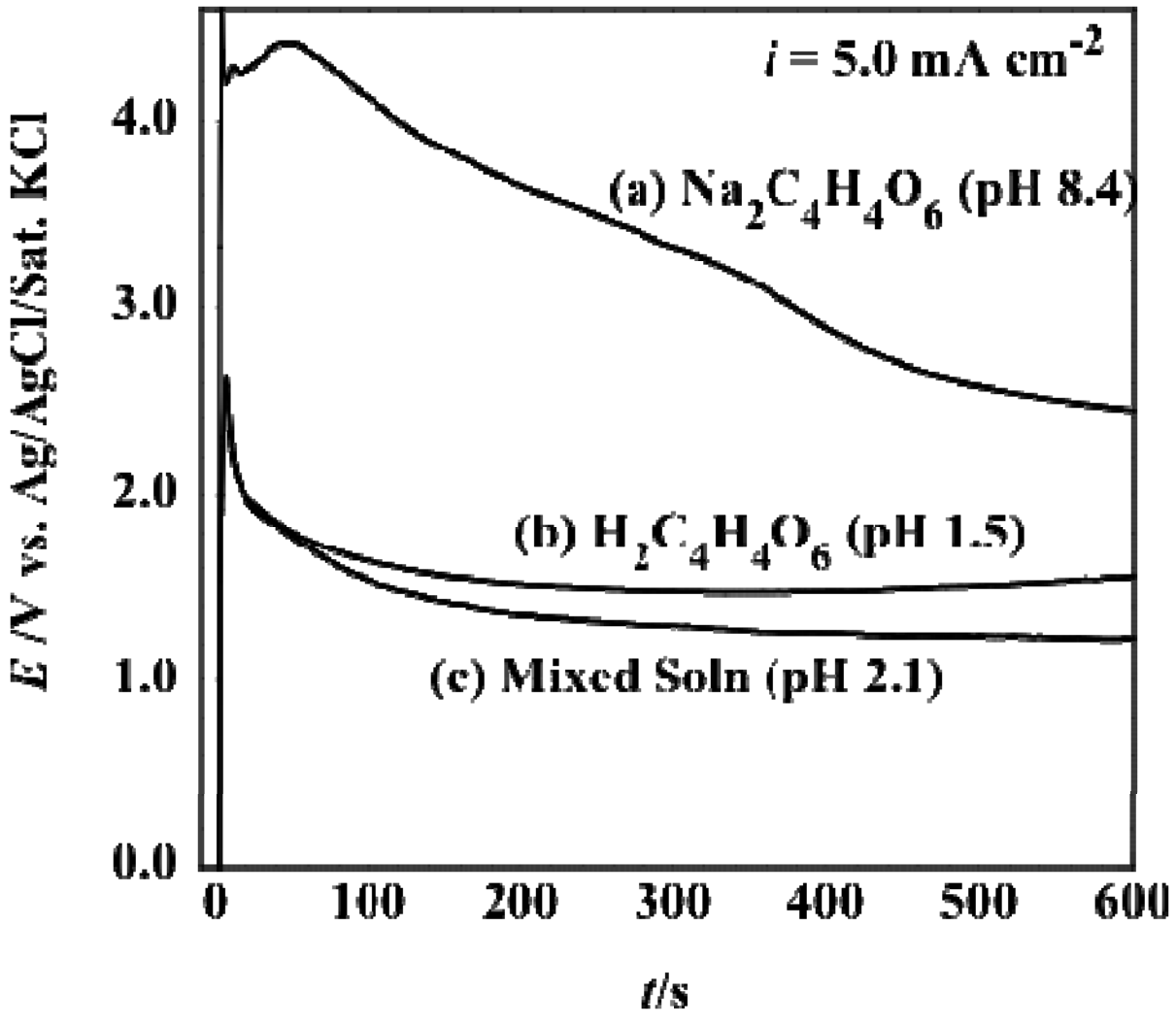
i = 5.0 mA cm-2
(a) Na2C4H4O6 (pH 8.4)
(b) H2C4H4O6 (pH 1.5)
(c) Mixed Soln (pH 2.1)
E /V vs. Ag/AgCl/Sat. KCl
4.0
3.0
2.0
1.0
0.0
0
100
200
300
400
500
600
t/s

Fig. 1

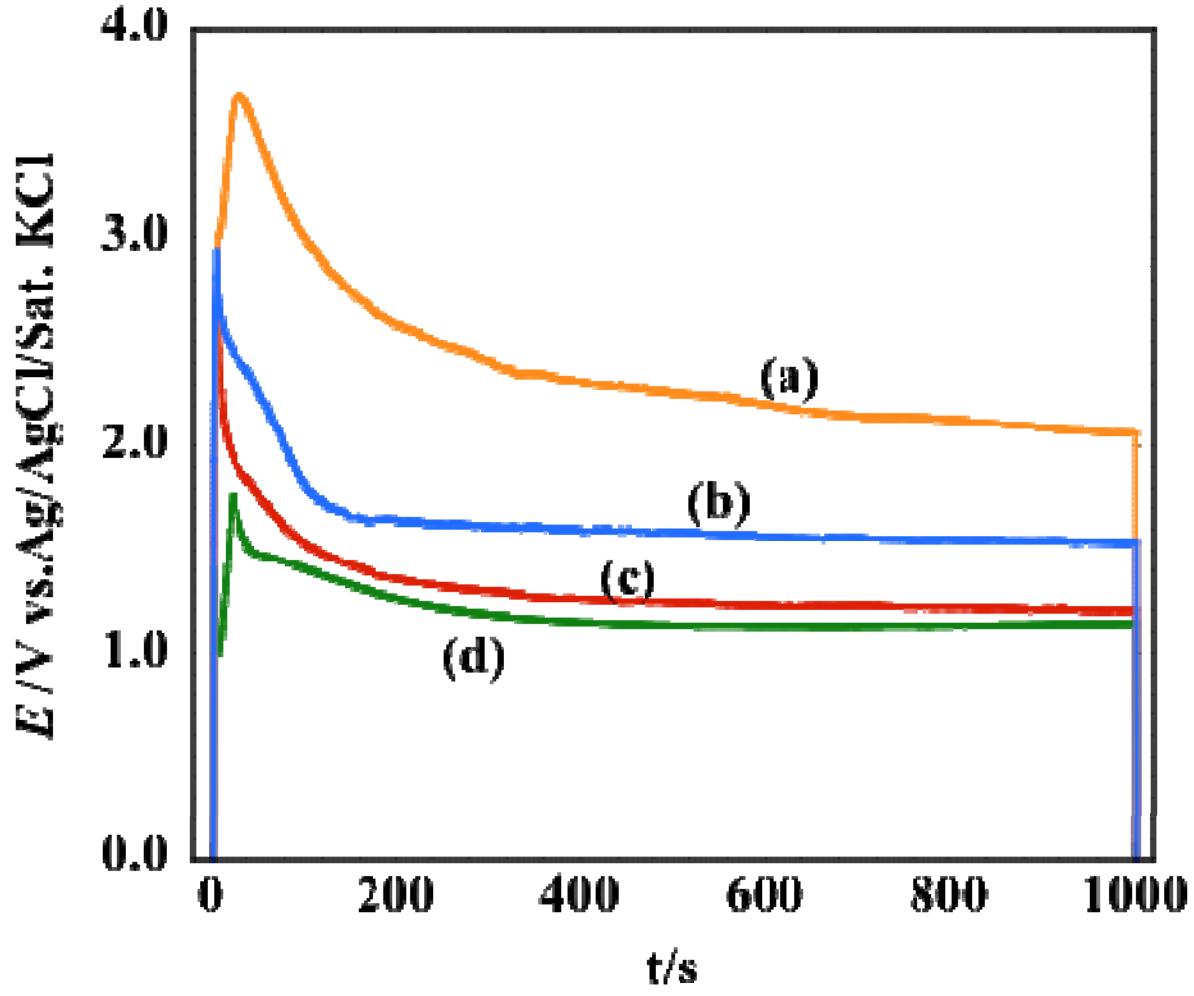

Fig. 2

(A)

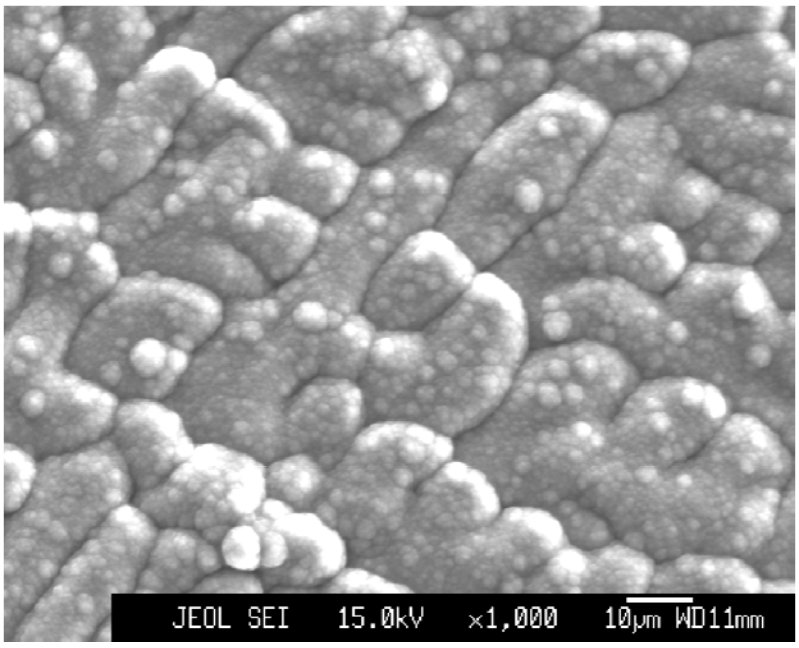
JEOL SEI 15.0kV ×1,000 10μm WD11mm

(B)

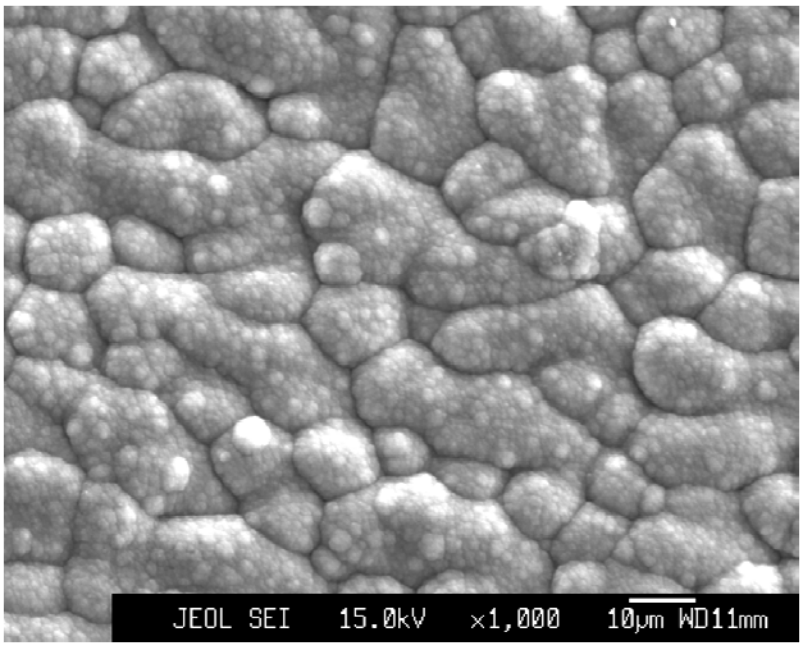
JEOL SEI 15.0kV ×1,000 10μm WD11mm

10μm

Fig. 3

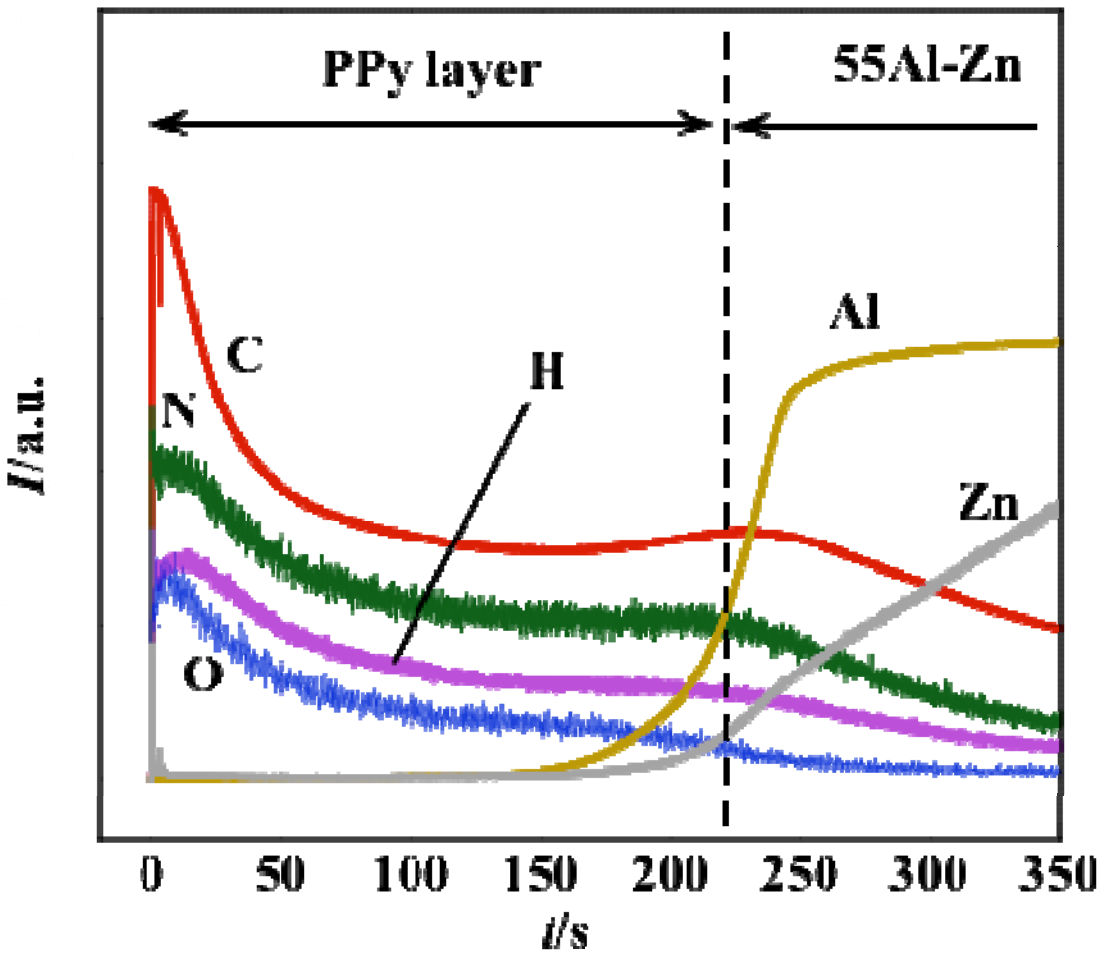

Fig. 4

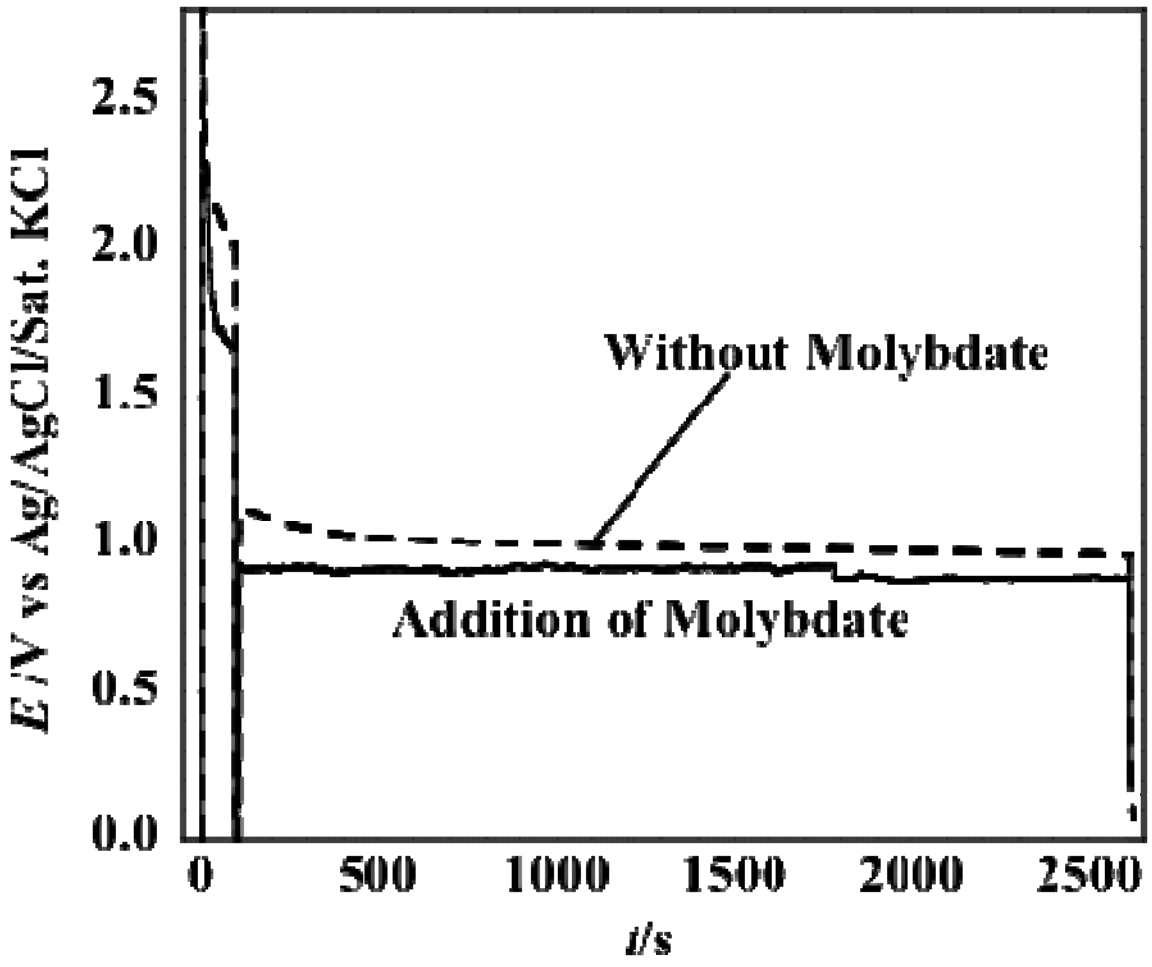
2.5
2.0
1.5
1.0
0.5
0.0
E /V vs Ag/AgCl/Sat. KCl
Without Molybdate
Addition of Molybdate
0
500
1000
1500
2000
2500
t/s

Fig. 5

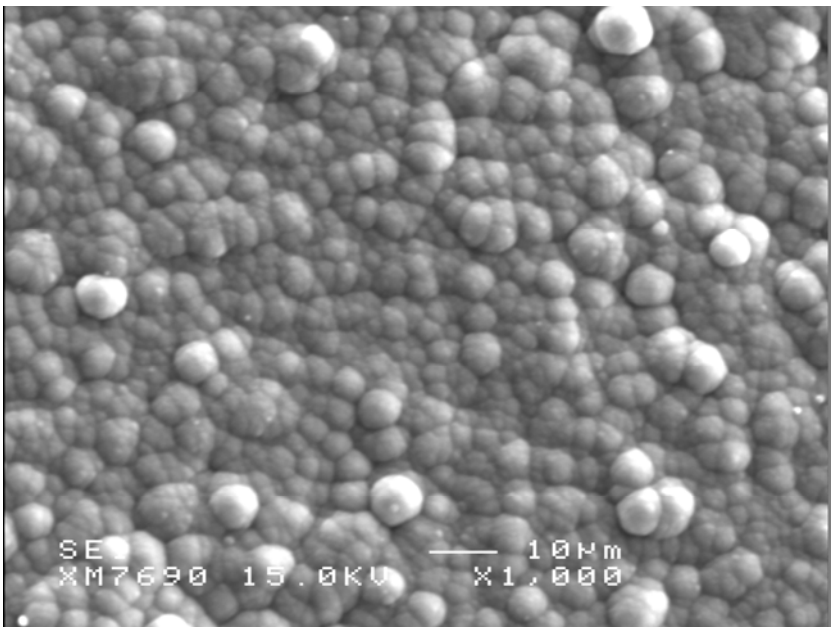

Fig. 6

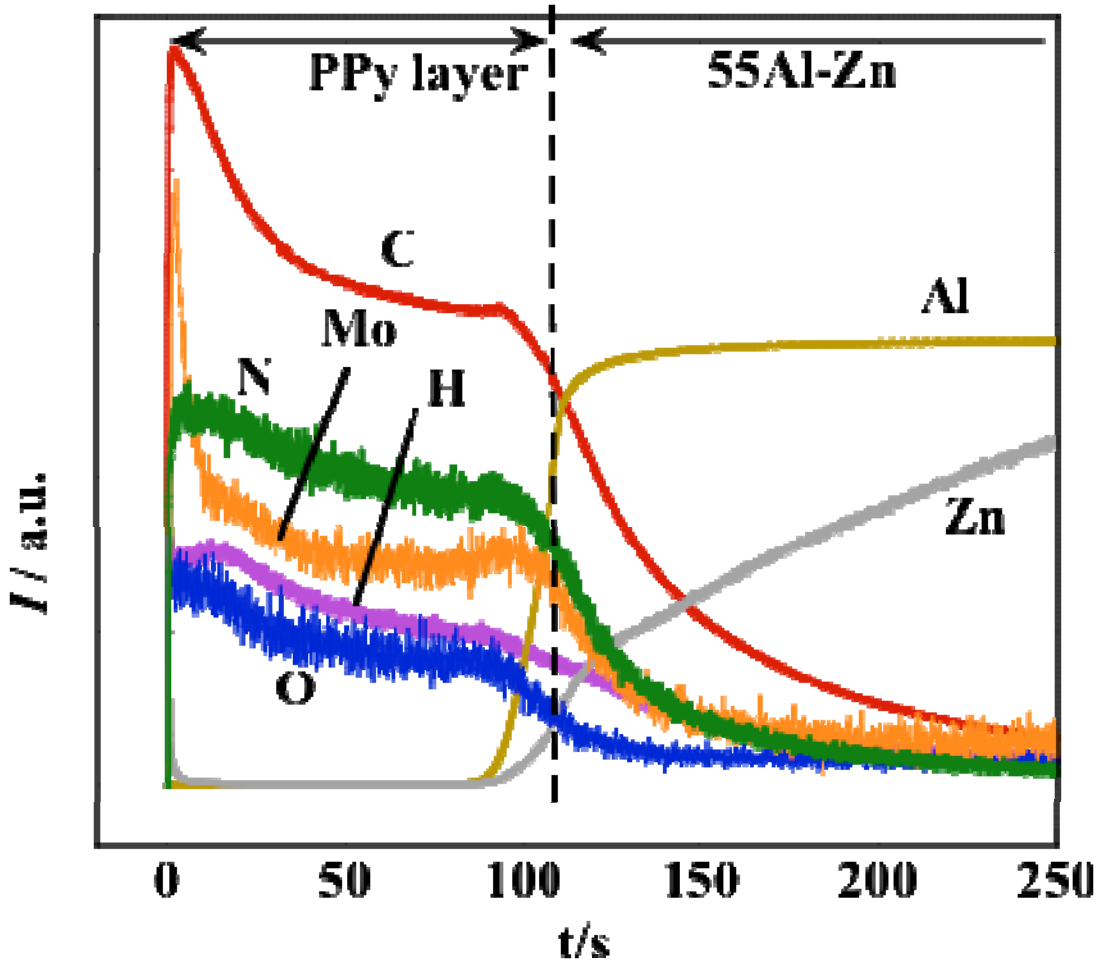

Fig. 7

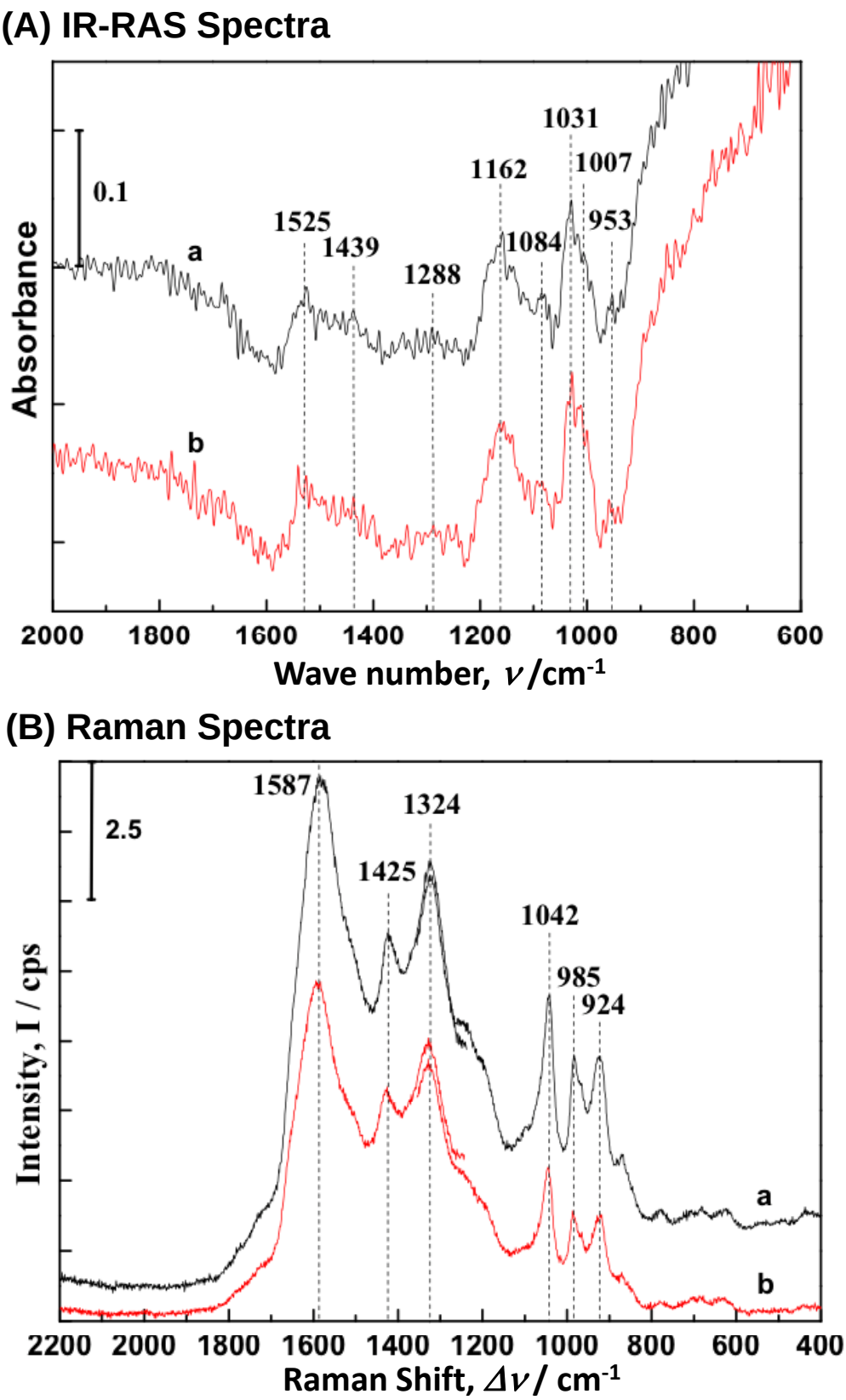
(A) IR-RAS Spectra
Absorbance
0.1
a
b
1525
1439
1288
1162
1084
1031
1007
953
2000
1800
1600
1400
1200
1000
800
600
Wave number, ν /cm-1
(B) Raman Spectra
Intensity, I / cps
2.5
1587
1324
1425
1042
985
924
a
b
2200
2000
1800
1600
1400
1200
1000
800
600
400
Raman Shift, Δν / cm-1

Fig. 8

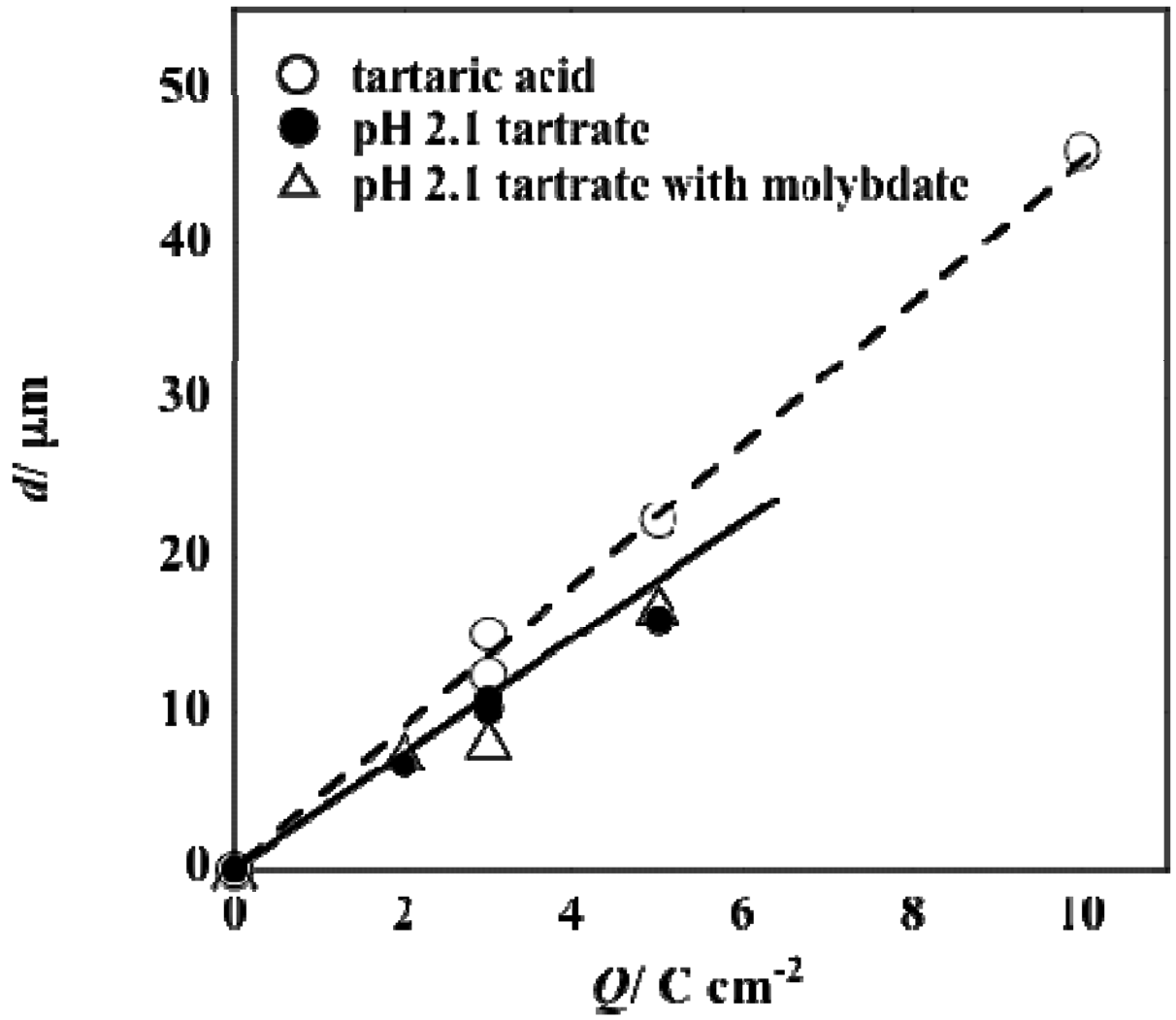
tartaric acid
pH 2.1 tartrate
pH 2.1 tartrate with molybdate
d/ µm
Q/ C cm-2
0
10
20
30
40
50
0
2
4
6
8
10

Fig. 9

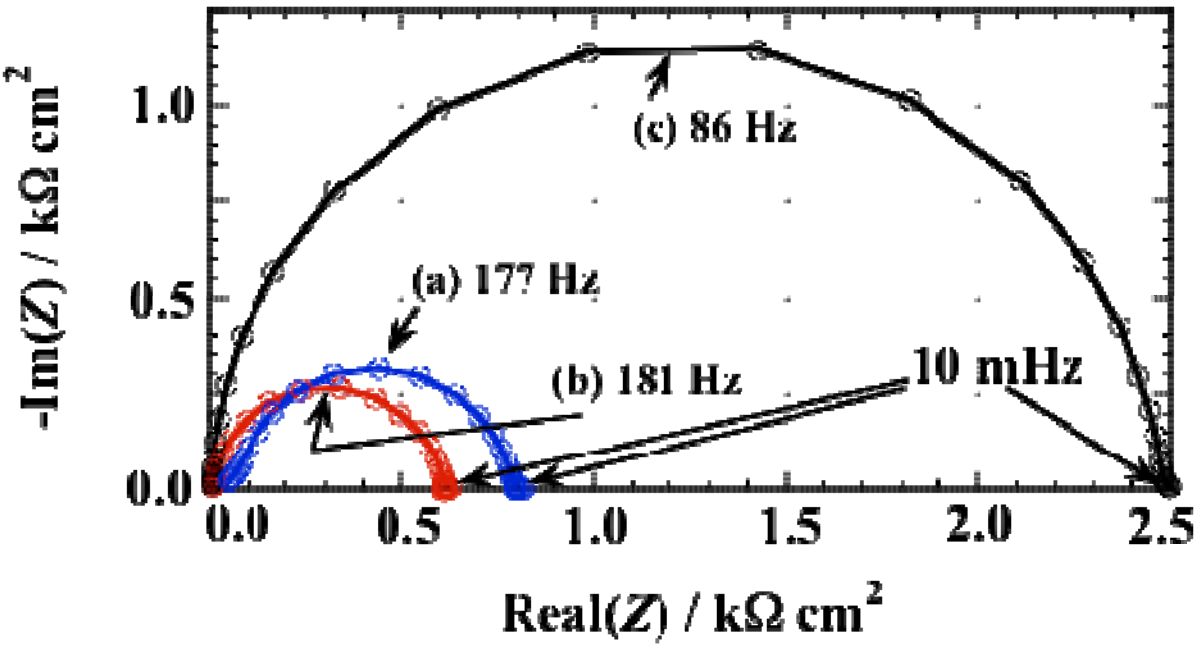
-Im(Z) / kΩ cm²
1.0
0.5
0.0
0.0
0.5
1.0
1.5
2.0
2.5
Real(Z) / kΩ cm²
(c) 86 Hz
(a) 177 Hz
(b) 181 Hz
10 mHz

Fig. 10

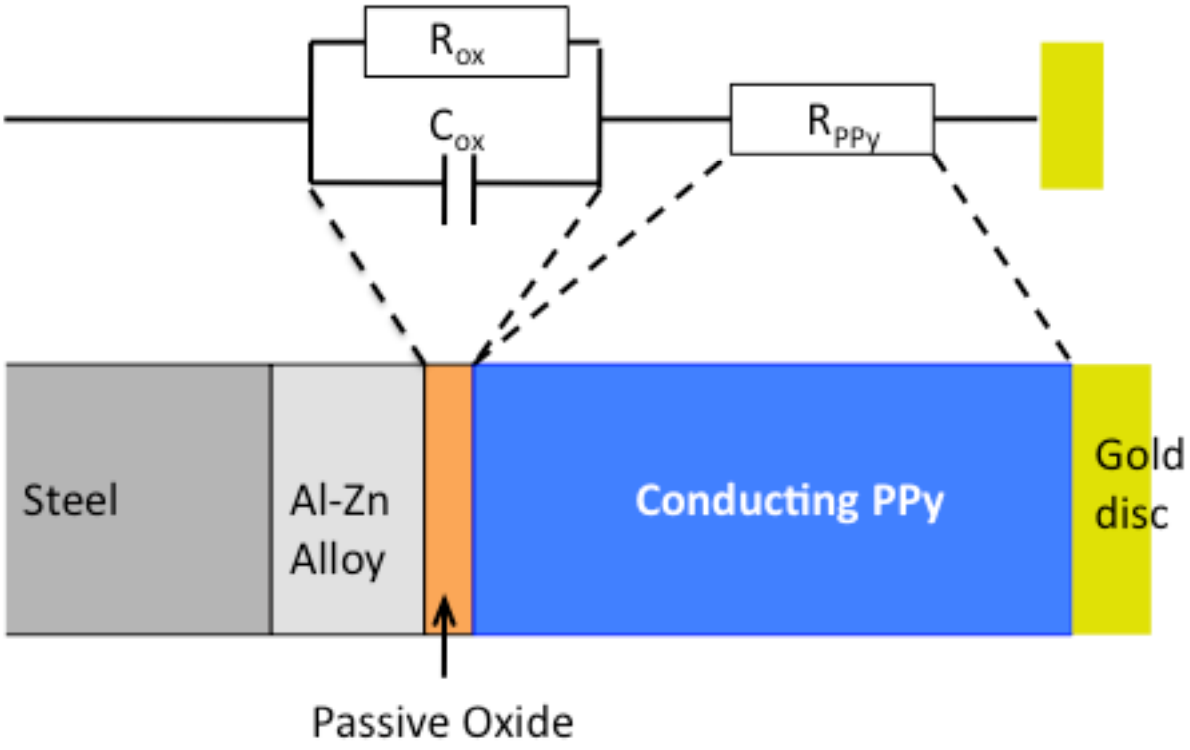
R_{ox}
C_{ox}
R_{PPy}
Steel
Al-Zn
Alloy
Conducting PPy
Gold
disc
Passive Oxide

Fig. 11

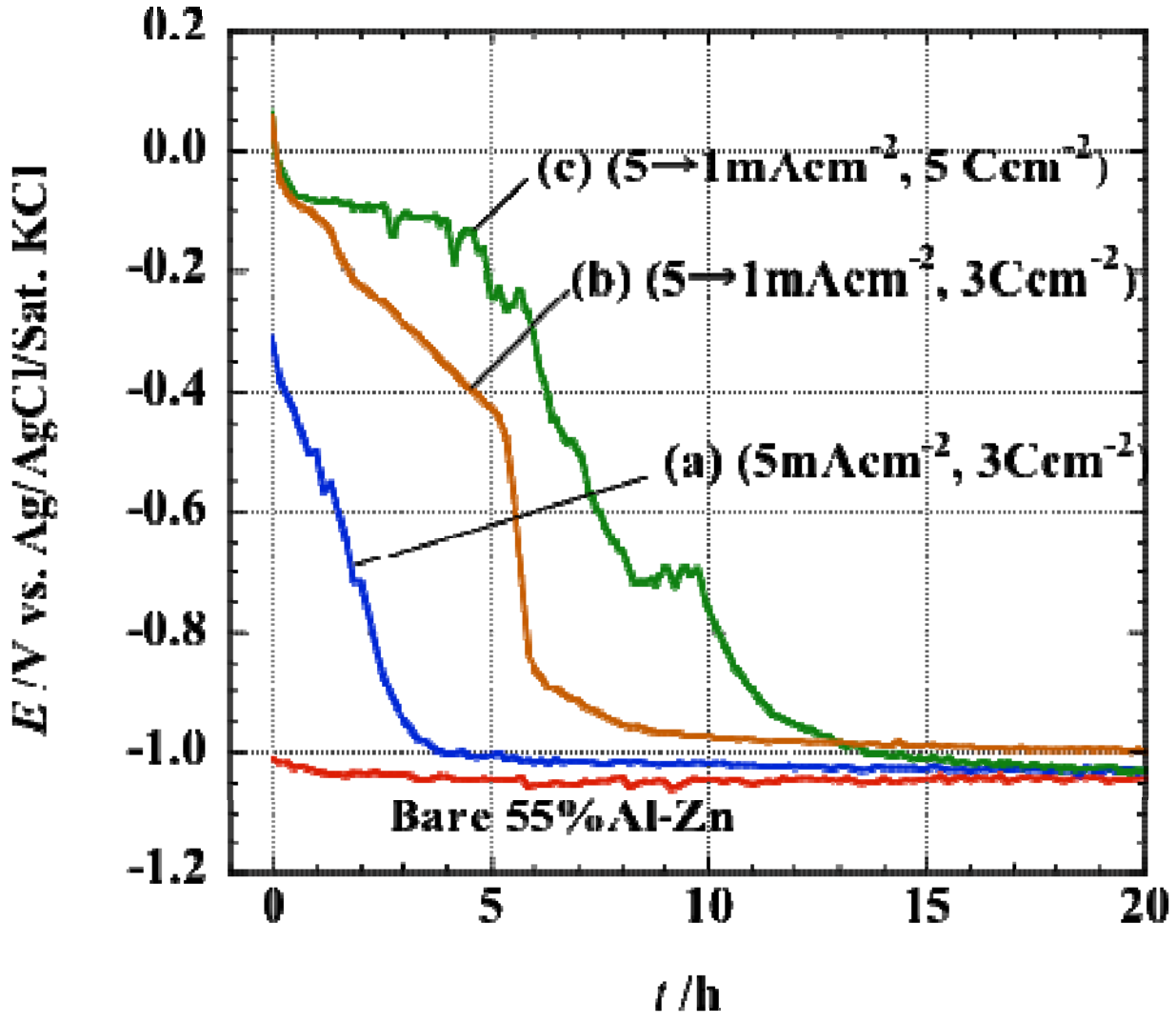
0.2
0.0
-0.2
-0.4
-0.6
-0.8
-1.0
-1.2
0
5
10
15
20
E /V vs. Ag/AgCl/Sat. KCl
t /h
(c) (5→1mAcm-2, 5 Ccm-2)
(b) (5→1mAcm-2, 3Ccm-2)
(a) (5mAcm-2, 3Ccm-2)
Bare 55%Al-Zn

Fig. 12

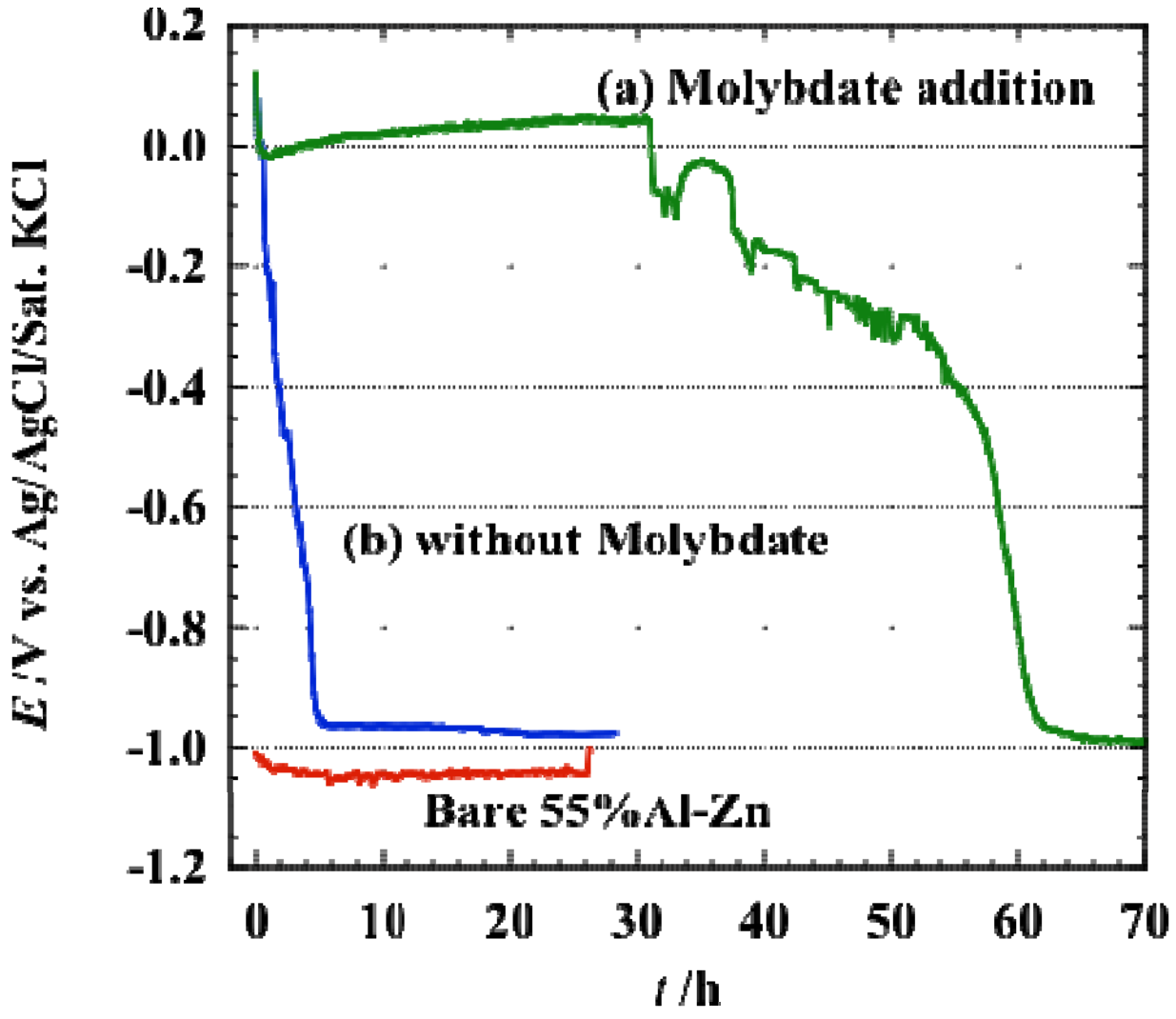
0.2
0.0
-0.2
-0.4
-0.6
-0.8
-1.0
-1.2
E /V vs. Ag/AgCl/Sat. KCl
(a) Molybdate addition
(b) without Molybdate
Bare 55%Al-Zn
0
10
20
30
40
50
60
70
t /h

Fig. 13

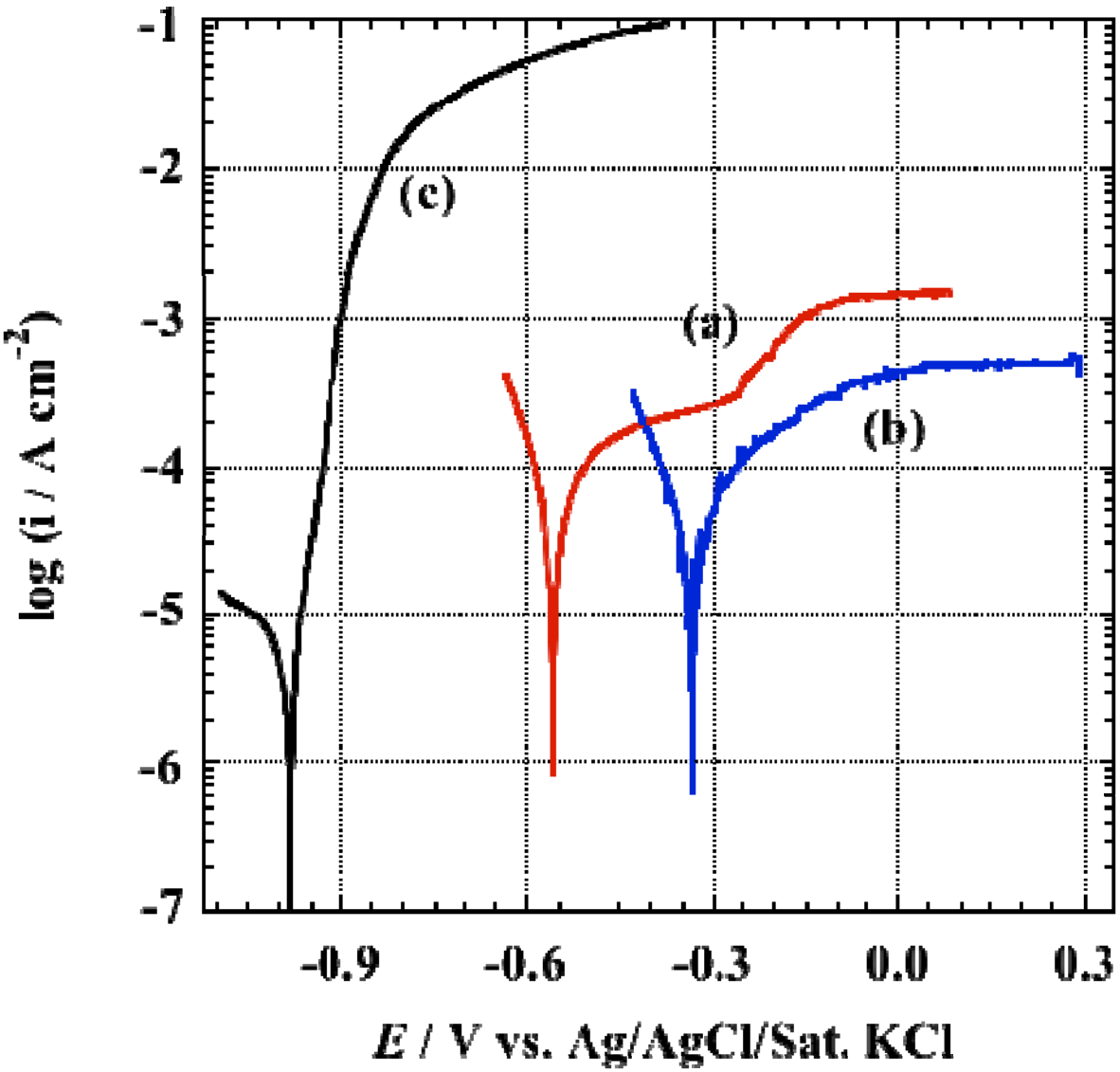

Fig. 14

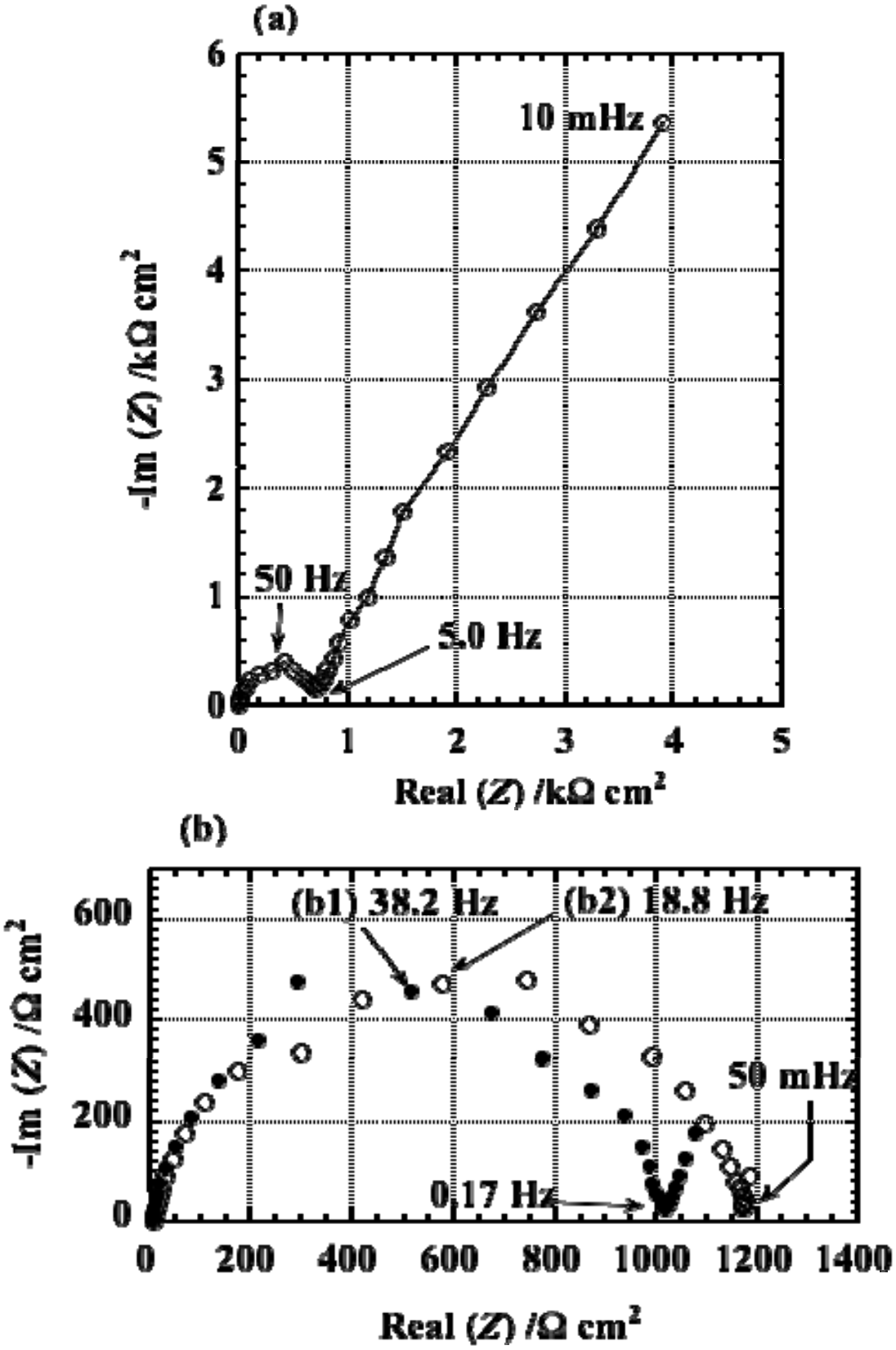
(a)
10 mHz
50 Hz
5.0 Hz
-Im (Z) /kΩ cm²
Real (Z) /kΩ cm²
(b)
(b1) 38.2 Hz
(b2) 18.8 Hz
50 mHz
0.17 Hz
-Im (Z) /Ω cm²
Real (Z) /Ω cm²

Fig. 15

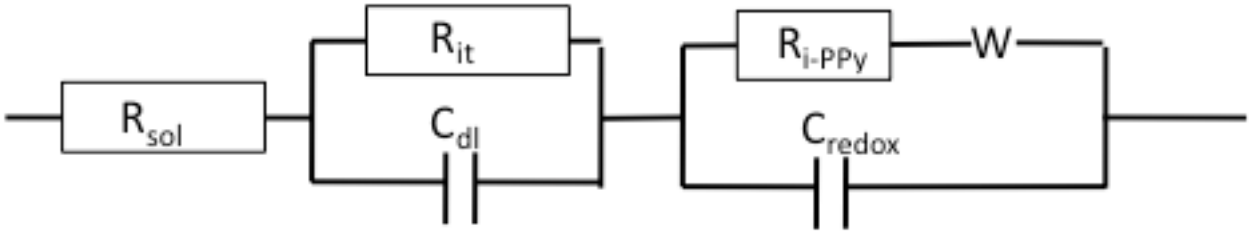

Fig. 16

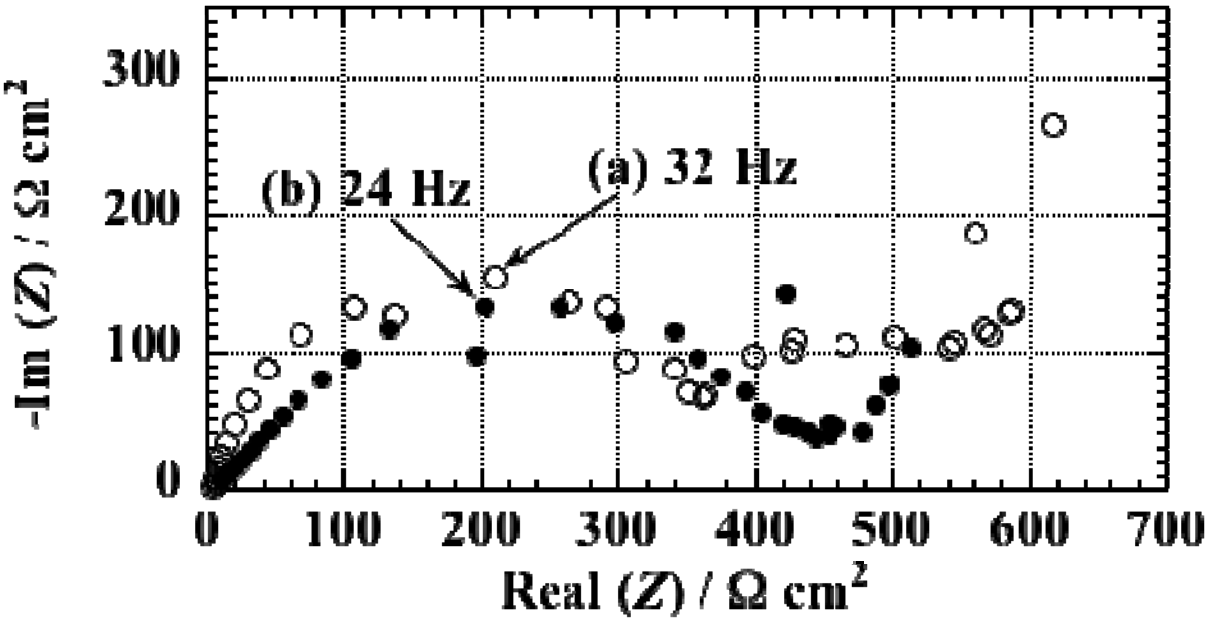
300
200
100
0
-Im (Z) / Ω cm²
(b) 24 Hz
(a) 32 Hz
0
100
200
300
400
500
600
700
Real (Z) / Ω cm²

Fig. 17

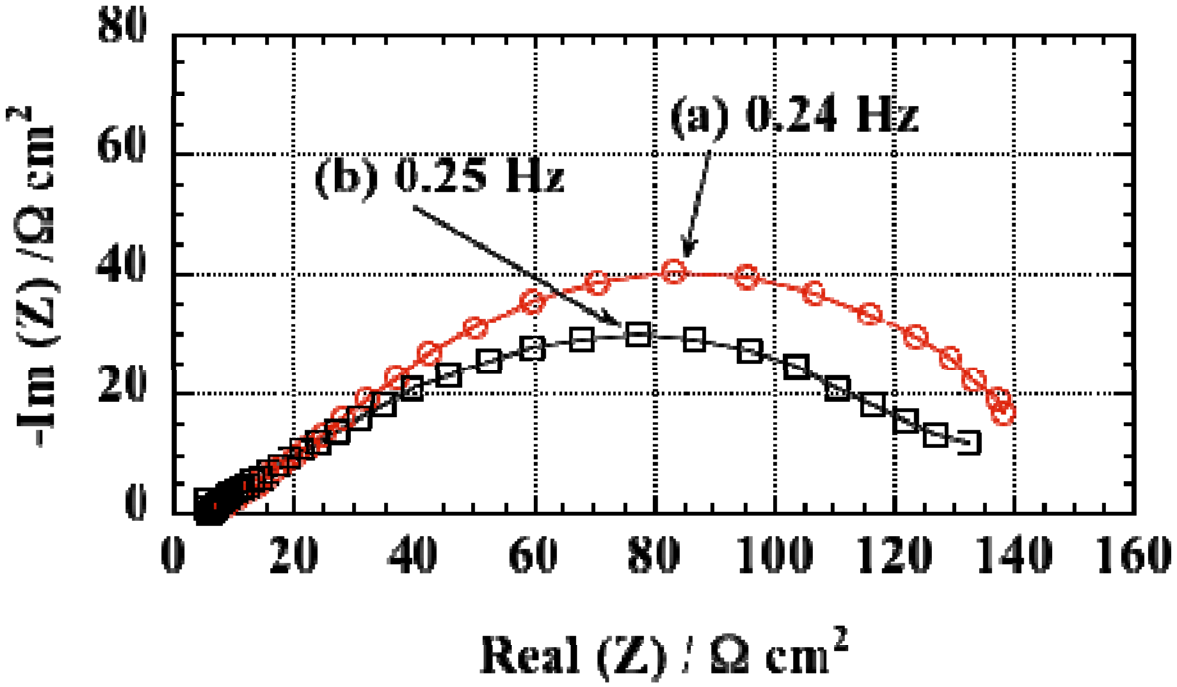
80
60
40
20
0
0
20
40
60
80
100
120
140
160
-Im (Z) /Ω cm²
Real (Z) / Ω cm²
(a) 0.24 Hz
(b) 0.25 Hz

Fig. 18

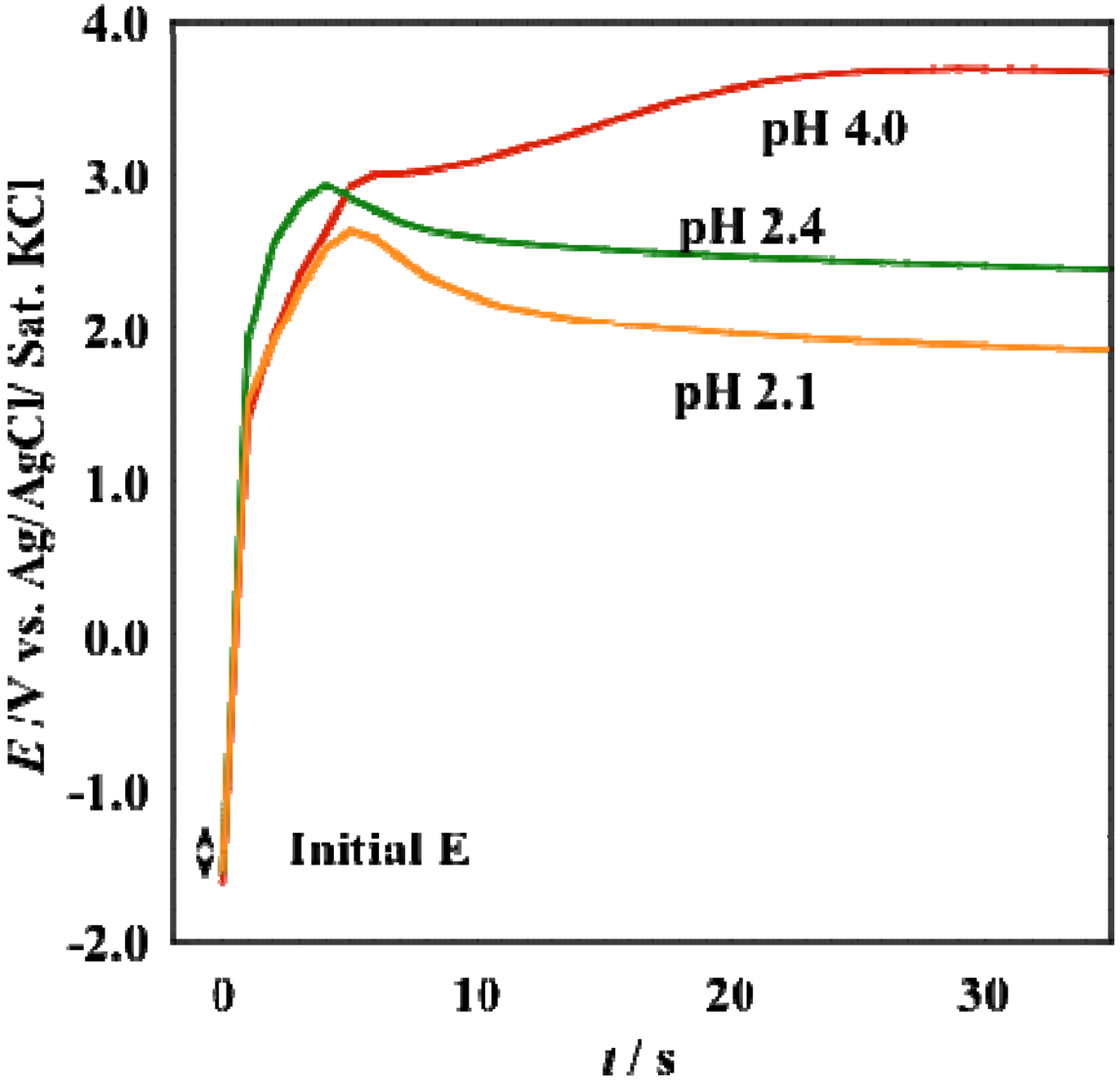
4.0
3.0
2.0
1.0
0.0
-1.0
-2.0
E /V vs. Ag/AgCl/ Sat. KCl
pH 4.0
pH 2.4
pH 2.1
Initial E
0
10
20
30
t / s

Fig. 19

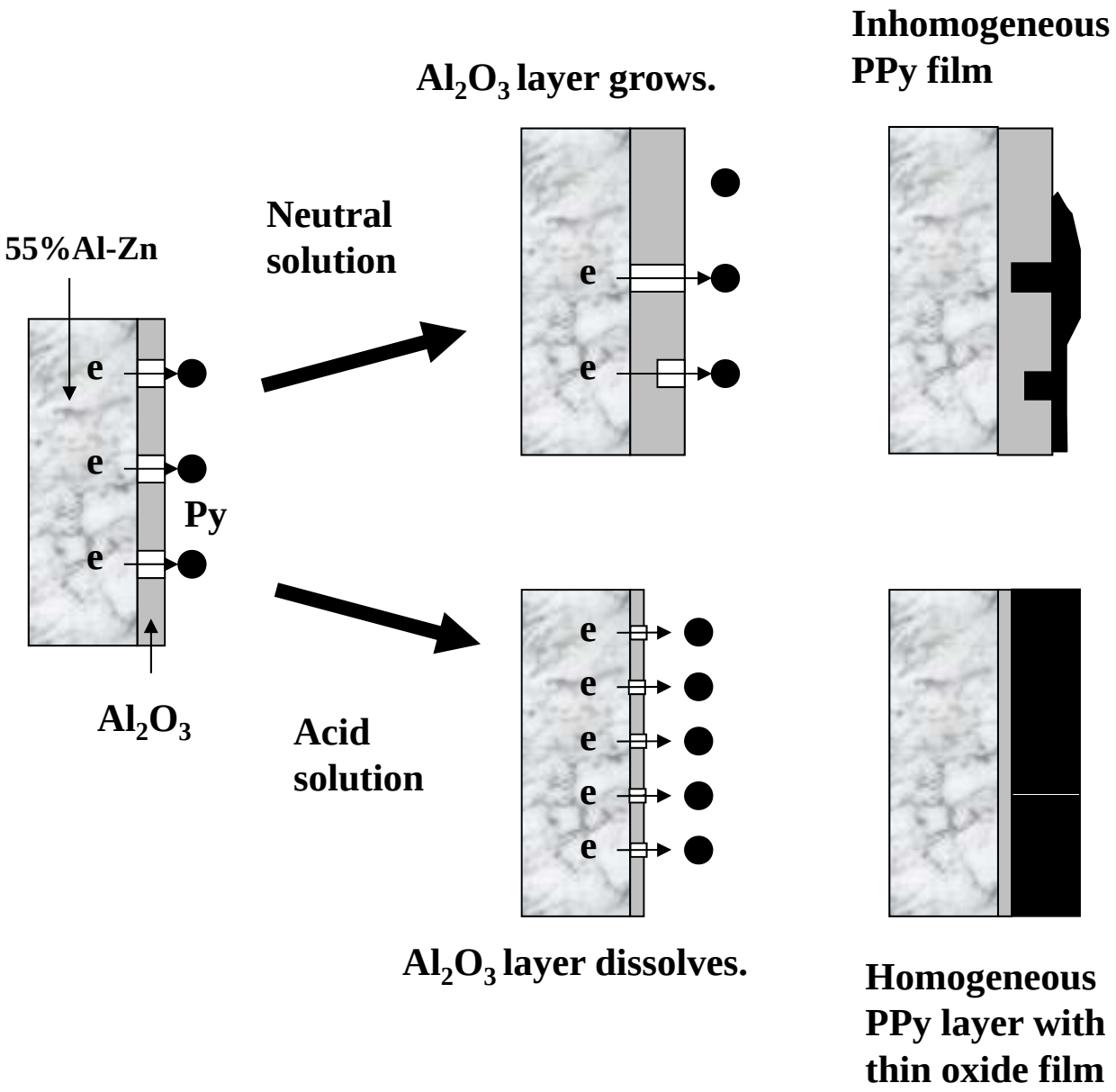
Inhomogeneous
PPy film
Al_2O_3 layer grows.
55%Al-Zn
Neutral
solution
e
e
e
Py
Al_2O_3
Acid
solution
e
e
e
e
e
Al_2O_3 layer dissolves.
Homogeneous
PPy layer with
thin oxide film

Fig. 20